Supporting Information

A self-assembled liquid crystal honeycomb of highly stretched (3-1-1)-hexagons

Alexander Scholte[1], Sebastian Hauche[1], Matthias Wagner[1], Marko Prehm[1], Silvio Poppe[1], Changlong Chen[2], Feng Liu[2], Xiangbing Zeng[3], Goran Ungar[2,3], Carsten Tschierske[1]

[1] Department of Chemistry, Martin Luther University Halle-Wittenberg, Kurt-Mothes-Str. 2, 06120 Halle, Germany
[2] State Key Laboratory for Mechanical Behaviour of Materials, Shaanxi International Research Center for Soft Matter, Xi'an Jiaotong University, Xi'an 710049, P.R. China
[3] Department of Materials Science and Engineering, Sheffield University, Sheffield S1 3JD, UK

Content

1. Experimental techniques…… S2

1.1 XRD…… ...S2
1.2 POM and DSC…… S3

2. Additional data…….. S3

2.1 Compound **1/22**……..S4
2.2 Compound **1/24**……S5
2.3 Compound **1/26**…….. S9
2.4 Compound **1/28**……..S9
2.5 Compound **1/30**……...S12
2.6 Compound **1/32**…… S13
2.7 Compound **1/34**…… S15
2.8 Structural data…… ..S18

3. Synthesis and analytical data…… S19

3.1 General…… S19
3.2 Synthesis of long chain alkyl bromides and intermediates……..… S19
3.3 Analytical data of compounds **1/22-1/34**……S23
3.4 Representative NMR spectra……. S26

4. References……. S27

1. Experimental techniques

1.1 XRD

X-ray scattering on aligned samples. - X-ray investigations were carried out at Cu Kα line (λ = 1.54 Å) using a standard Coolidge tube source with a Ni-filter. Aligned samples were obtained on a glass plate on a temperature-controlled heating stage. Alignment was achieved upon slow cooling (rate: 1 K·min^{-1} – 0.01 K·min^{-1}) of a small droplet of the sample and takes place at the sample–glass or at the sample–air interface. The diffraction patterns were recorded with a 2D detector (Vantec 500, Bruker); the exposure time was 15 min for WAXS and 30 min for SAXS. The beam was parallel to the substrate.

Synchrotron X-ray diffraction and electron density reconstruction. High-resolution small-angle powder diffraction experiments were recorded on Beamline I22 at Diamond Light Source and Beamline BL16B1 at Shanghai Synchrotron Radiation Facility, SSRF. Samples were held in evacuated 1 mm capillaries. A modified Linkam hot stage with a thermal stability within 0.2 ºC was used, with a hole for the capillary drilled through the silver heating block and mica windows attached to it on each side. A MarCCD detector was used. q calibration and linearization were verified using several orders of layer reflections from silver behemate and a series of n-alkanes. The measurement of the positions and intensities of the diffraction peaks is carried out using Galactic PeakSolve™ program, where experimental diffractograms are fitted using Gaussian shaped peaks. The diffraction peaks are indexed on the basis of their peak positions, and the lattice parameters and the space groups are subsequently determined. Once the diffraction intensities are measured and the corresponding space group determined, 3-d electron density maps can be reconstructed, on the basis of the general formula

$$E(xy) = \Sigma_{hk} F(hk) \exp[\mathrm{i}2\pi(hx+ky)] \qquad \text{(Eqn. 1)}$$

Here $F(hk)$ is the structure factor of a diffraction peak with index (hk). It is normally a complex number and the experimentally observed diffraction intensity.

$$I(hk) = \mathrm{K}\cdot F(hk)\cdot F^*(hk) = \mathrm{K}\cdot|F(hk)|^2 \qquad \text{(Eqn. 2)}$$

Here K is a constant related to the sample volume, incident beam intensity etc. In this paper we are only interested in the relative electron densities, hence this constant is simply taken to be 1. Thus the electron density

$$E(xy) = \Sigma_{hk} \mathrm{sqrt}[I(hk)] \exp[i2\pi(hx+ky) + \phi_{hk}] \qquad \text{(Eqn. 3)}$$

As the observed diffraction intensity $I(hk)$ is only related to the amplitude of the structure factor $|F(hk)|$, the information about the phase of $F(hk)$, ϕ_{hk}, can not be determined directly from experiment. However, the problem is much simplified when the structure of the ordered phase is centrosymmetric, and hence the structure factor $F(hk)$ is always real and ϕ_{hk} is either 0 or π.

This makes it possible for a trial-and-error approach, where candidate electron density maps are reconstructed for all possible phase combinations, and the "correct" phase combination is then selected on the merit of the maps, helped by prior physical and chemical knowledge of the system. This is especially useful for the study of nanostructures, where normally only a limited number of diffraction peaks are observed.

GISAXS experiments were carried out on station BM28 (XMaS line) at ESRF. Thin films were prepared from the melt on a silicon wafer. The thin film coated 5 x 5 mm^2 Si plates were placed on top of a custom built heater, which was then mounted on a six-circle goniometer. A MarCCD 165 detector at ESRF was used. The sample enclosure and the beam pipe were flushed with helium.

1.2 POM and DSC

Polarizing Optical Microscopy (POM). Transition temperatures were measured using a Mettler FP-82 HT hot stage and control unit in conjunction with a Leica DMRXP polarizing microscope (Leica Microsystems GmbH, Wetzlar, Germany). Textures of the liquid crystalline mesophases were recorded with a Leica MC120 HD camera (Leica Microsystems GmbH, Wetzlar, Germany).

DSC measurements. DSC-thermograms were recorded on a DSC-7 (Perkin-Elmer) in 30 μL Al-pans with heating and cooling rates of 10 K min^{-1}.

2. Additional data

Table S1. Transition temperatures and associated enthalpies of the LC phase of compounds **1/22-1/34** as recorded on heating (H) and cooling (C)[a]

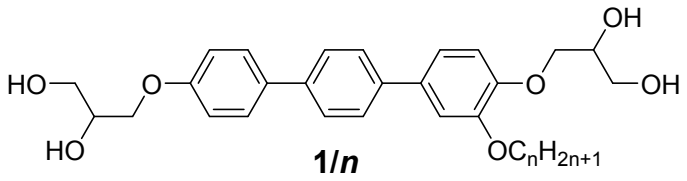

1/*n*

1/*n*	Phase transitions *T* /°C; [*ΔH* /kJ mol^{-1}]
1/22	H: Cr_1 91 [10.0] Cr_2 138 [29.2] Col_{hex}/*p6mm* 200 [10.7] Iso C: Iso 197 [-10.3] Col_{hex}/*p6mm* 54 [-20.6] Cr
1/24	H: Cr_1 90 [16.3] Cr_2 140 [10.6] Col_{rec}/*c2mm*(2-1-1) 186 [1.4] Lam_{Sm}/*p2mm* 196 [6.4] Iso C: Iso 193 [-6.2] Lam_{Sm}/*p2mm* 184 [-1.7] Col_{rec}/*c2mm*(2-1-1) 59 [-22.2] Cr
1/26	H: Cr_1 91 [17.0] Cr_2 141 [12.2] Col_{rec}/*c2mm*(2-1-1) 191 [1.7] Lam_{Sm}/*p2mm* 202 [6.5] Iso C: Iso 198 [-6.6] Lam_{Sm}/*p2mm* 187 [-3.0] Col_{rec}/*c2mm*(2-1-1) 59 [-21.7] Cr
1/28	H: Cr_1 90 [28.1] Cr_2 141 [10.9] Col_{rec}/*c2mm*(2-1-1) 191 [2.9] Lam_{Sm}/*p2mm* 206 [7.9] Iso C: Iso 203 [-7.2] Lam_{Sm}/*p2mm* 189 [-2.4] Col_{rec}/*c2mm*(2-1-1) 62 [-27.0] Cr
1/30	H: Cr_1 116 [24.0] Cr_2 138 [85.7] Col_{rec}/*c2mm*(2-1-1) 179 [2.7] Lam_{Sm} 201 [8.1] Iso C: Iso 196 [-7.1] Lam_{Sm} 173 [-2.5] Col_{rec}/*c2mm*(2-1-1) 64 [-30.2] Cr
1/32	H: Cr 142 [30.0] Col_{rec}/*c2mm*(2-1-1) 167 [2.9] Lam_{Sm}/*p2mm* 204 [8.2] Iso C: Iso 201 [-8.0] Lam_{Sm}/*p2mm* 164 [-2.7] Col_{rec}/*c2mm*(2-1-1) 70 [-32.3] Cr
1/34	H: Cr 142 [30.1] Col_{rec}/*c2mm*(3-1-1) 154 [2.3] Lam_{Sm}/*p2mm* 203 [8.3] Iso C: Iso 200 [-7.8] Lam_{Sm}/*p2mm* 150 [-2.4] Col_{rec}/*c2mm*(3-1-1) 71 [-29.7] Cr

[a] Data were taken from the first DSC heating and cooling scans at 10 K min^{-1} (peak temperatures).

2.1 Compound 1/22

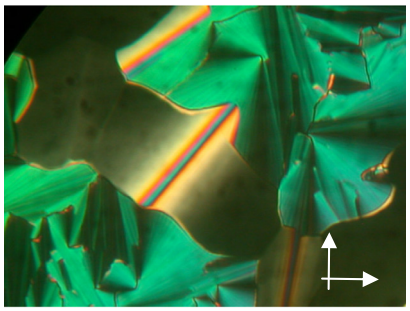

Figure S1. Texture of the *p6mm* phase of **1/22** at T = 180 °C, the dark areas are homeotropically aligned, i.e. the columns are perpendicular to the substrate surfaces.

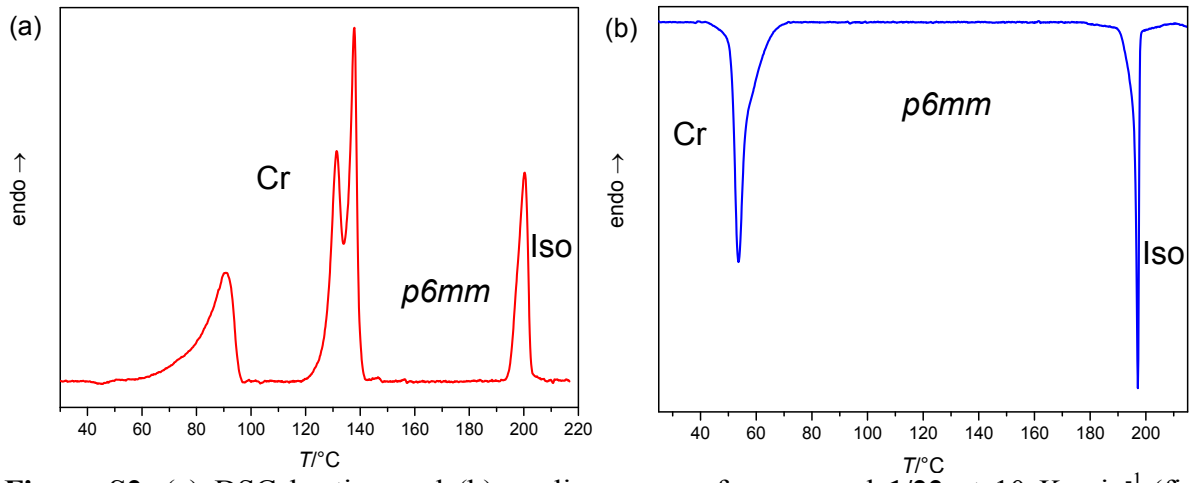

Figure S2. (a) DSC heating and (b) cooling scans of compound **1/22** at 10 K min^{-1} (first heating and cooling).

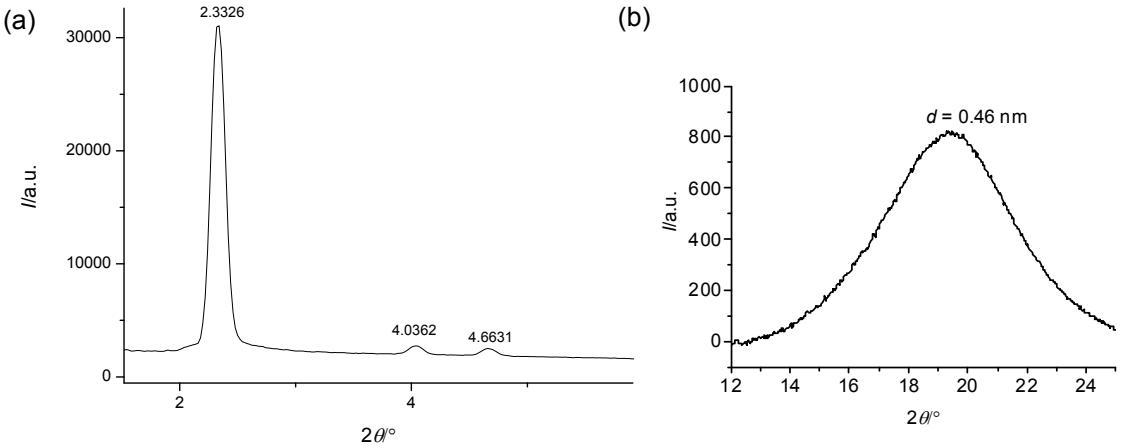

(*hk*)	$d_{obs.}$ – spacing (nm)	$d_{cal.}$ – spacing (nm)	$d_{obs} - d_{calc}$
(10)	3.79	3.79	0.00
(11)	2.19	2.19	0.00
(20)	1.90	1.89	0.01
a_{hex} = 4.37 nm			

Figure S3. (a) SAXS and (b) WAXS pattern and numerical crystallographic data of the Col_{hex} phase of **1/22** at 150 °C.

2.2 Compound 1/24

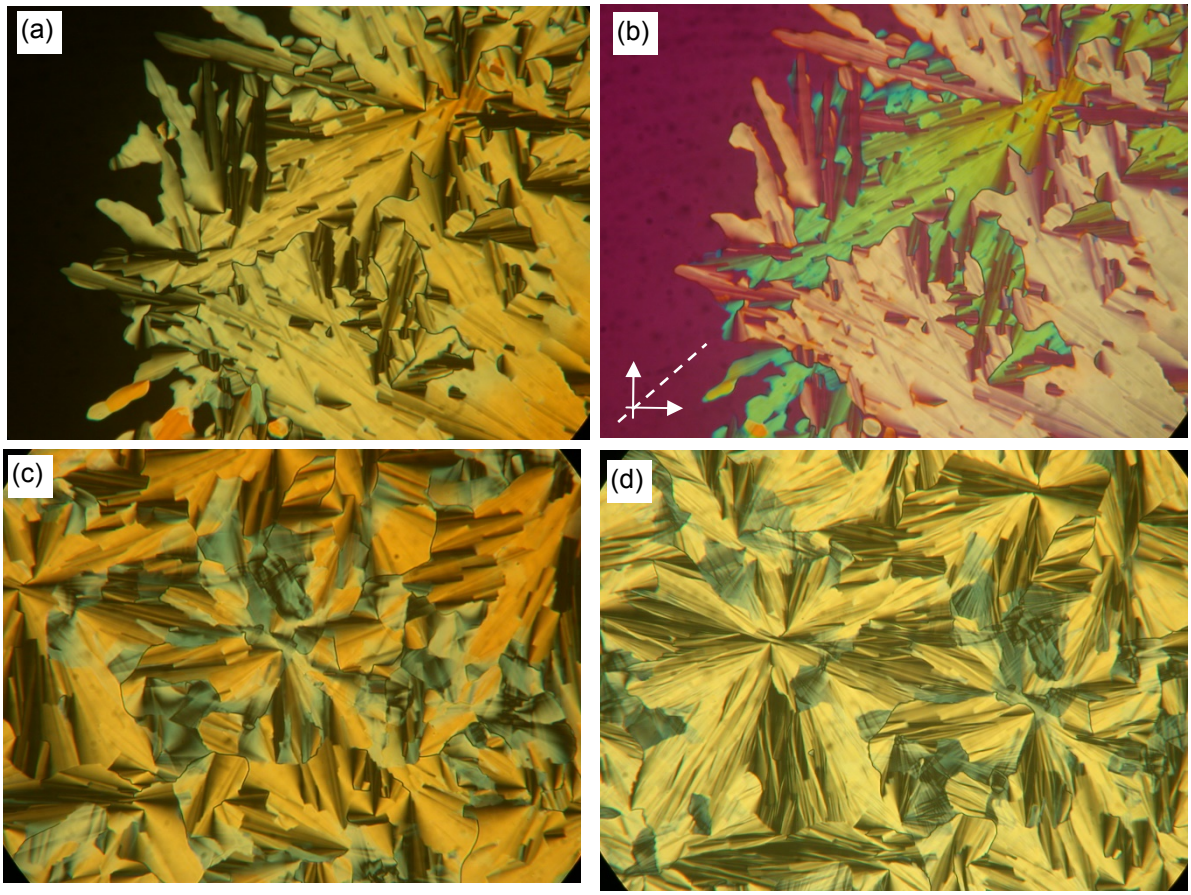

Figure S4. Textures of compound **1/24** as observed between crossed polarizers, (a,b) at the Iso-Lam$_{Sm}$/*p*2*mm* transition at T = 196 °C in (b) with λ retarder plate), (c) in the Lam$_{Sm}$/*p*2*mm* phase at T = 190 °C and (d) in the Col$_{rec}$/*c*2*mm*(2-1-1) phase at T = 170 °C (both without λ-plate). The directions of the polarizers (arrows) and the indicatrix (dashed line) of the λ-plate are shown in (b).

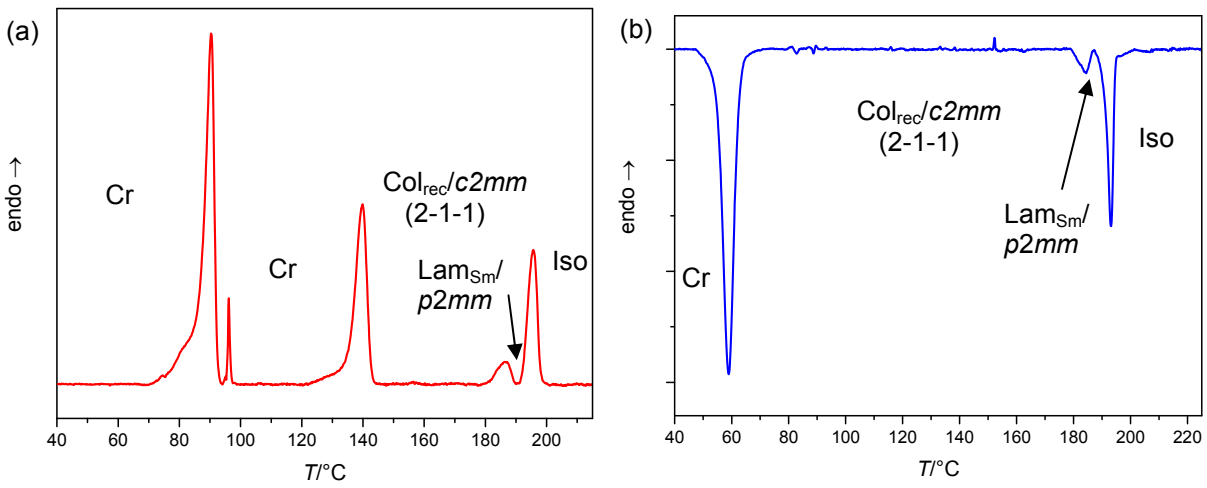

Figure S5. (a) DSC heating and (b) cooling scans of compound **1/24** at 10 K min^{-1} (second heating and cooling).

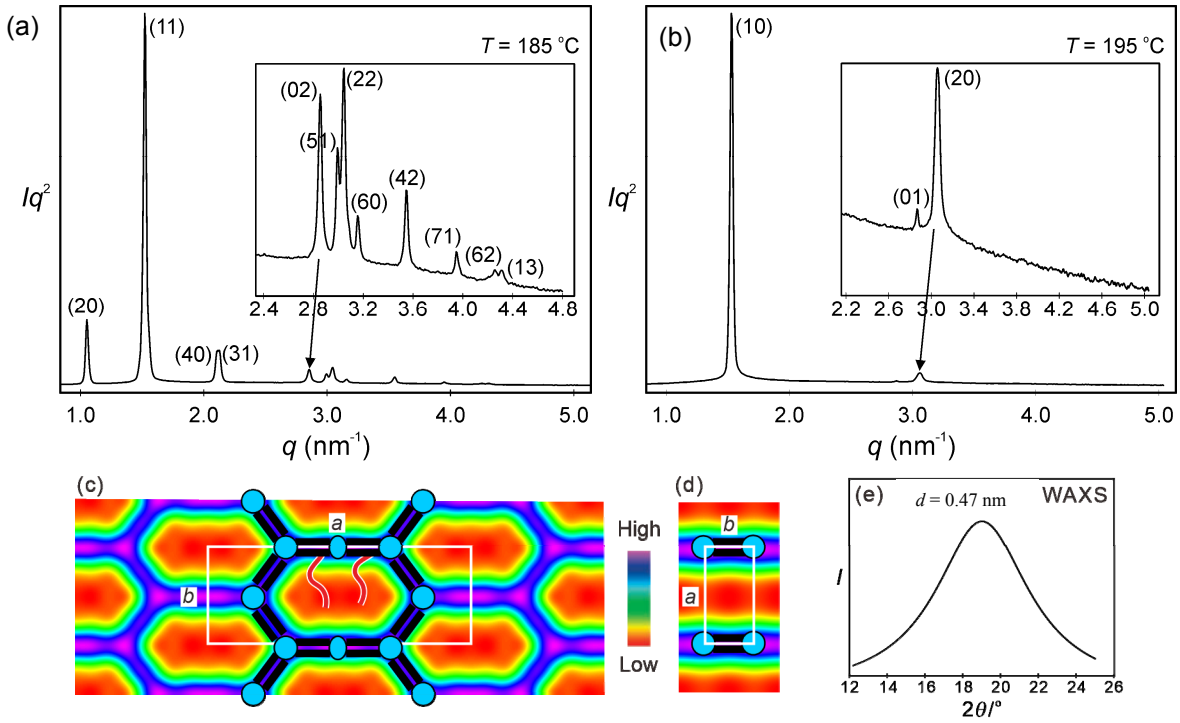

Figure S6. Powder diffraction pattern of **1/24** (a) in the *c*2*mm*(2-1-1) phase at T = 185 °C and (b) in the Lam_{Sm}/*p*2*mm* phase at T = 195°C (synchrotron source), (c,d) the corresponding ED maps and (e) the wide angle scan at T = 150 °C.

Table S2 Experimental and calculated *d*-spacings of the observed SAXS reflections of the rectangular phase *c*2*mm*(2-1-1) in compound **1/24** at 185 ºC. All intensities values are Lorentz and multiplicity corrected.

(*hk*)	$d_{obs.}$ – spacing (nm)	$d_{cal.}$ – spacing (nm)	*intensity*	*phase*
(20)	5.97	5.97	30.8	π
(11)	4.13	4.13	100.0	π
(40)	2.98	2.99	14.3	0
(31)	2.95	2.95	7.4	0
(02)	2.20	2.20	8.1	0
(51)	2.10	2.10	2.8	π
(22)	2.07	2.06	4.5	0
(60)	1.99	1.99	1.6	π
(42)	1.77	1.77	1.9	π
(71)	1.59	1.59	0.6	0
(62)	1.48	1.48	0.4	0
(13)	1.46	1.46	0.4	π
a_{rec} = 11.94 nm, b_{rec} = 4.40 nm				

Table S3 Experimental and calculated *d*-spacings of the observed SAXS reflections of the Lam_{Sm}/*p2mm* in compound **1/24** at 195 ºC. All intensities values are Lorentz and multiplicity corrected.

(*hk*)	$d_{obs.}$ – spacing (nm)	$d_{cal.}$ – spacing (nm)	*intensity*	*phase*
(10)	4.11	4.11	100.0	π
(01)	2.19	2.19	0.2	π
(20)	2.05	2.05	4.4	0
a_{rec} = 4.11 nm, b_{rec} = 2.19 nm				

2.3 Compound 1/26

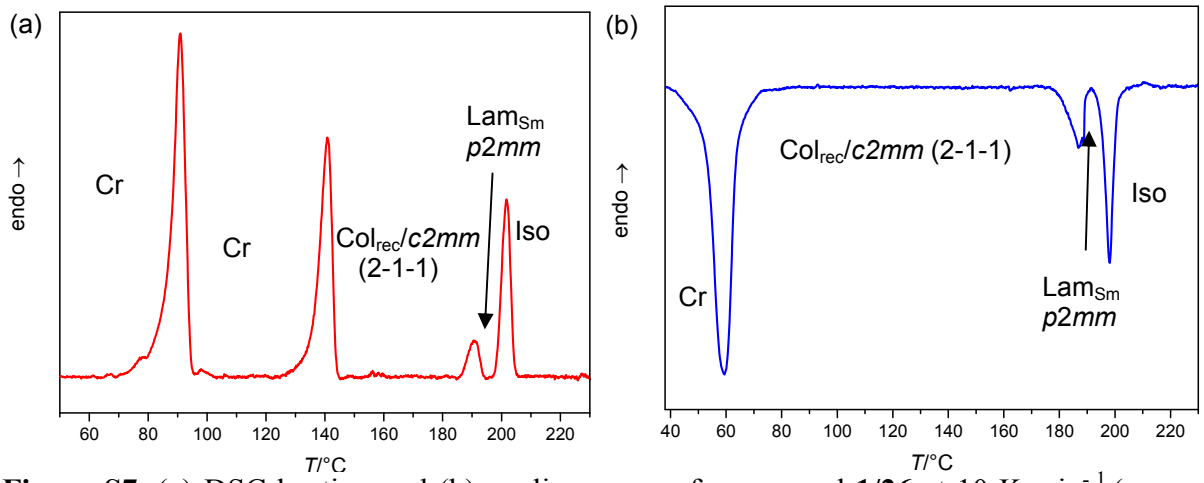

Figure S7. (a) DSC heating and (b) cooling scans of compound **1/26** at 10 K min^{-1} (second heating and cooling).

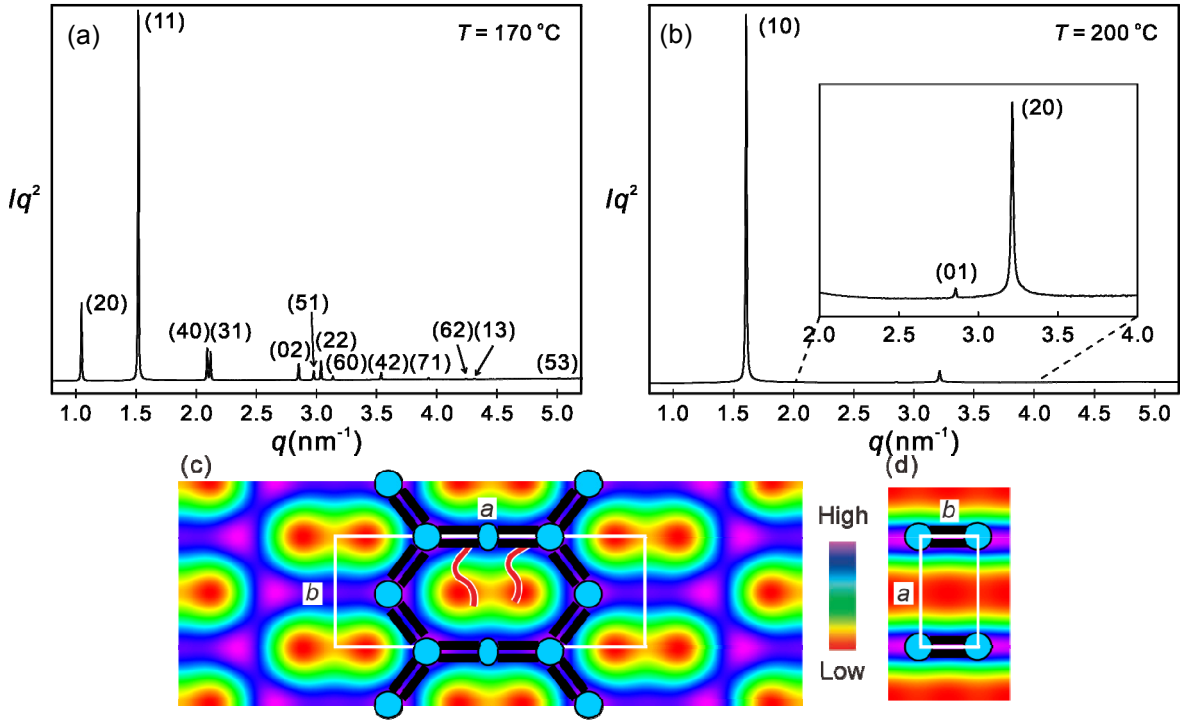

Figure S8. SAXS diffractograms of compound **1/26** (a) in the Col_{rec}/*c2mm*(2-1-1) phase at 170 ºC and (b) in the Lam_{Sm}/*p2mm* phase at 200 ºC with the corresponding electron density maps shown in (c) and (d), respectively.

Table S4. Experimental and calculated *d*-spacings, relative integrated intensities, and phases used in the reconstruction of electron densities for the $Col_{rec}/c2mm$(2-1-1) phase of **1/26** at 170 ºC. All intensities values are Lorentz and multiplicity corrected.

(*hk*)	$d_{obs.}$- spacings (nm)	$d_{cal.}$- spacings (nm)	*Intensity*	*Phase*
(20)	6.01	6.01	42.1	π
(11)	4.14	4.14	100.0	π
(40)	3.01	3.01	16.5	0
(31)	2.97	2.97	7.1	0
(02)	2.20	2.21	9.0	0
(51)	2.11	2.11	2.5	π
(22)	2.07	2.07	5.1	0
(60)	2.00	2.00	1.8	π
(42)	1.78	1.78	2.1	π
(71)	1.60	1.60	0.5	0
(62)	1.48	1.48	0.2	0
(13)	1.46	1.46	0.2	π
(53)	1.25	1.25	0.1	π
a_{rec} = 12.02 nm, b_{rec} = 4.41 nm				

Table S5. Experimental and calculated *d*-spacings, relative integrated intensities, and phases used in the reconstruction of electron densities for the $Lam_{Sm}/p2mm$ phase of **1/26** at 200 ºC. All intensities values are Lorentz and multiplicity corrected.

(*hk*)	$d_{obs.}$- spacings (nm)	$d_{cal.}$- spacings (nm)	*Intensity*	*Phase*
(10)	3.91	3.91	100.0	π
(01)	2.20	2.20	0.1	π
(20)	1.96	1.96	4.0	0
a_{rec} = 3.91 nm, b_{rec} = 2.20 nm				

2.4 Compound 1/28

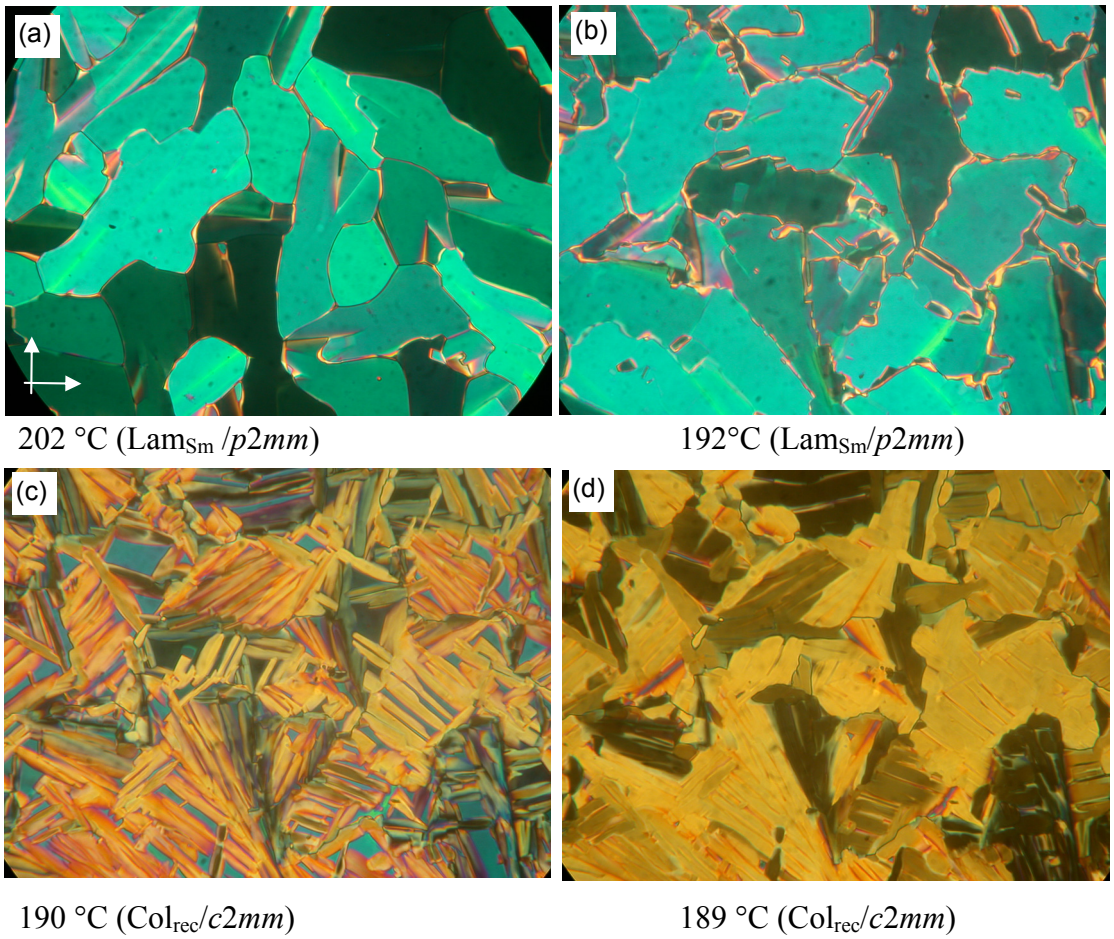

202 °C (Lam_{Sm} /*p2mm*) 192°C (Lam_{Sm}/*p2mm*)

190 °C (Col_{rec}/*c2mm*) 189 °C (Col_{rec}/*c2mm*)

Figure S9. Mosaic-like textures of compound **1/28** as observed between crossed polarizers at the indicated temperatures; the decreases from (b) to (d) at the phase transition from Lam_{Sm}/*p2mm* to Col_{rec}/*c2mm*.

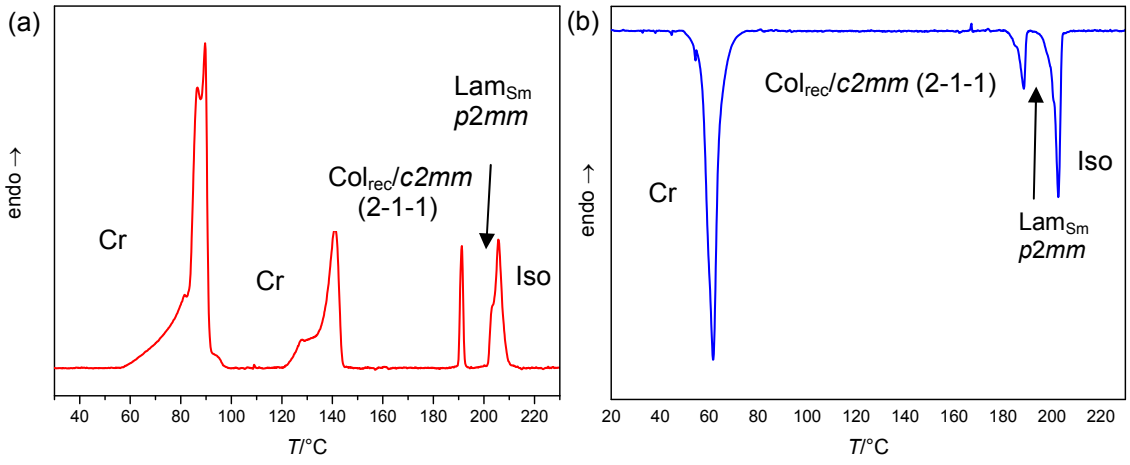

Figure S10. (a) DSC heating and (b) cooling scans of compound **1/28** at 10 K min^{-1} (first heating and cooling).

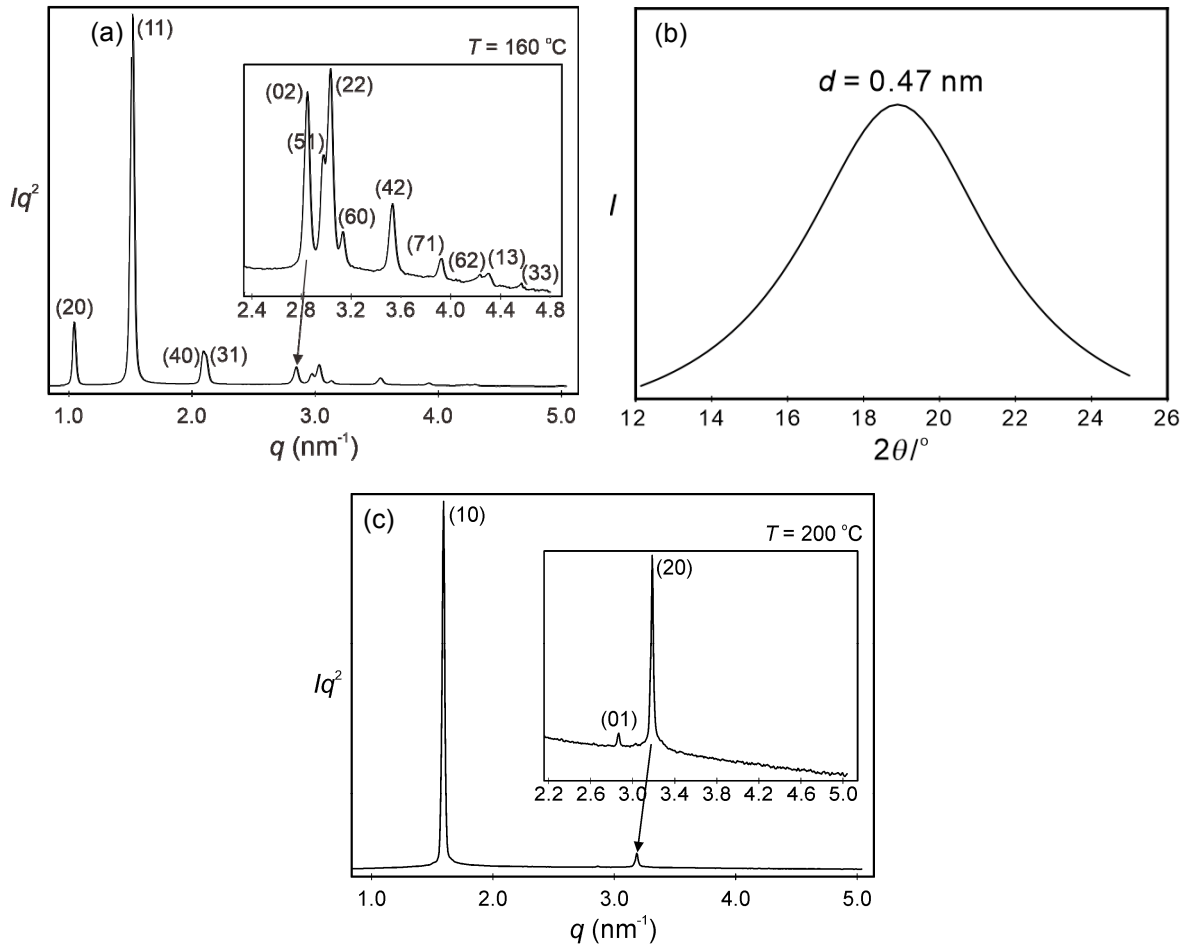

Figure S11. Compound **1/28:** (a) and (b) SAXS and WAXS diffractogram of the $Col_{rec}/c2mm$(2-1-1) phase at 160 ºC; (c) SAXS diffractogram of the $Lam_{Sm}/p2mm$ phase at T = 200 °C.

Table S6. Experimental and calculated *d*-spacings of the observed SAXS reflections of the rectangular phase *c*2*mm*(2-1-1) in compound **1/28** at 160 ºC. All intensities values are Lorentz and multiplicity corrected.

(*hk*)	$d_{obs.}$ – spacing (nm)	$d_{cal.}$ – spacing (nm)	*intensity*	*phase*
(20)	6.01	6.01	28.2	π
(11)	4.14	4.14	100.0	π
(40)	3.00	3.01	14.0	0
(31)	2.97	2.97	6.7	0
(02)	2.21	2.21	10.8	0
(51)	2.11	2.11	3.4	π
(22)	2.07	2.07	5.8	0
(60)	2.00	2.00	2.2	π
(42)	1.78	1.78	2.3	π
(71)	1.60	1.60	0.6	0
(62)	1.48	1.48	0.4	0
(13)	1.46	1.46	0.4	π
(33)	1.38	1.38	0.1	0
a_{rec} = 12.03 nm, b_{rec} = 4.41 nm				

Table S7. Experimental and calculated *d*-spacings of the observed SAXS reflections of the rectangular phase Lam_{Sm}/*p*2*mm* in compound **1/28** at 200 ºC. All intensities values are Lorentz and multiplicity corrected.

(*hk*)	$d_{obs.}$ – spacing (nm)	$d_{cal.}$ – spacing (nm)	*intensity*	*phase*
(10)	3.95	3.95	100.0	π
(01)	2.19	2.19	0.2	π
(20)	1.97	1.97	3.9	0
a_{rec} = 3.95 nm, b_{rec} = 2.19 nm				

2.5 Compound 1/30

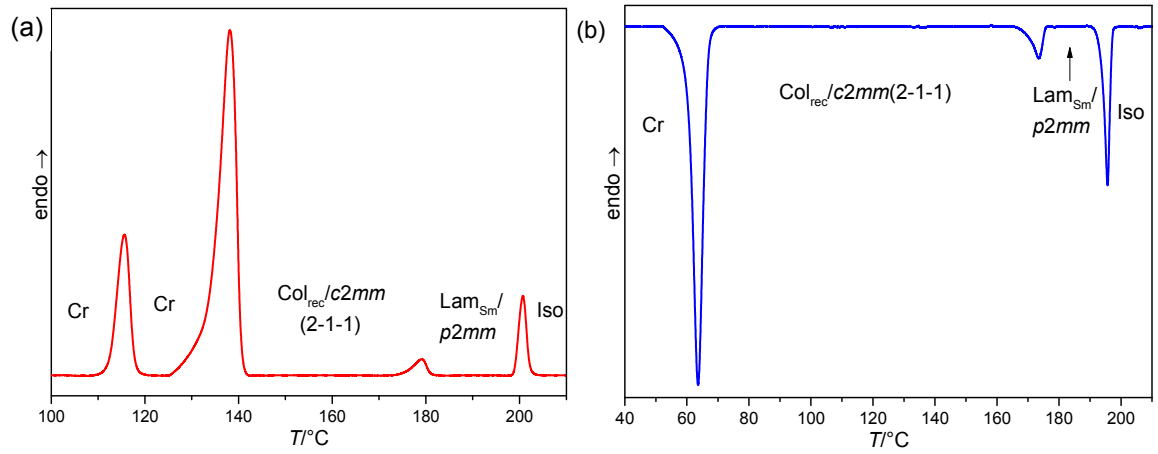

Figure S12. (a) DSC heating and (b) cooling scans of compound **1/30** at 10 K min^{-1} (first heating and cooling).

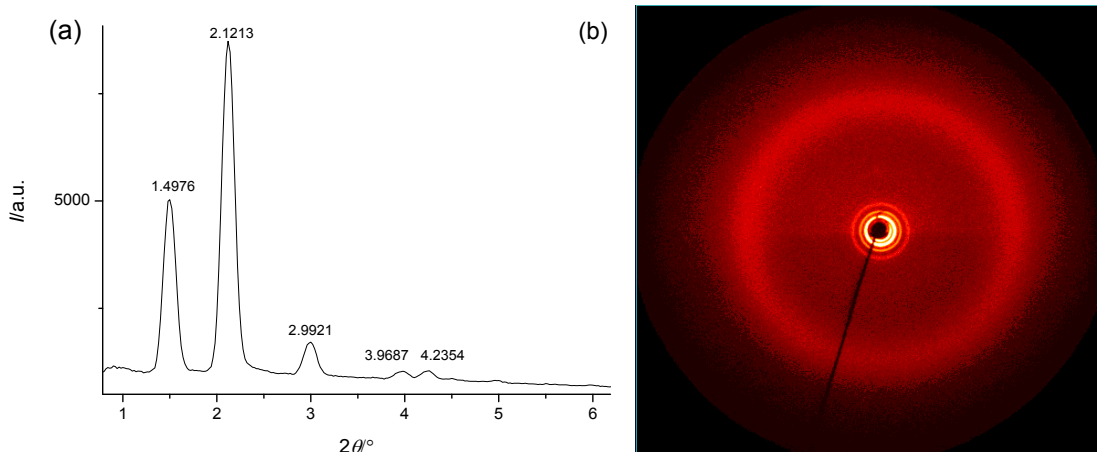

Figure S13. (a) SAXS pattern and (b) WAXS of **1/30** in the *c*2*mm*(2-1-1) phase at T = 160 °C

Table S8. Reflections of the Col$_{rec}$/*c*2*mm*(2-1-1) in compound **1/30** at 160 ºC.

(*hk*)	d_{obs} – spacings (nm)	d_{calc} – spacings (nm)	$d_{obs} - d_{calc}$
(02)	5.90	5.90	0.00
(11)	4.17	4.17	0.00
(04)	2.95	2.95	0.00
(20)	2.23	2.23	0.00
(15)	2.09	2.09	0.00
a_{rec} = 11.80 nm, b_{rec} = 4.45 nm			

2.6 Compound 1/32

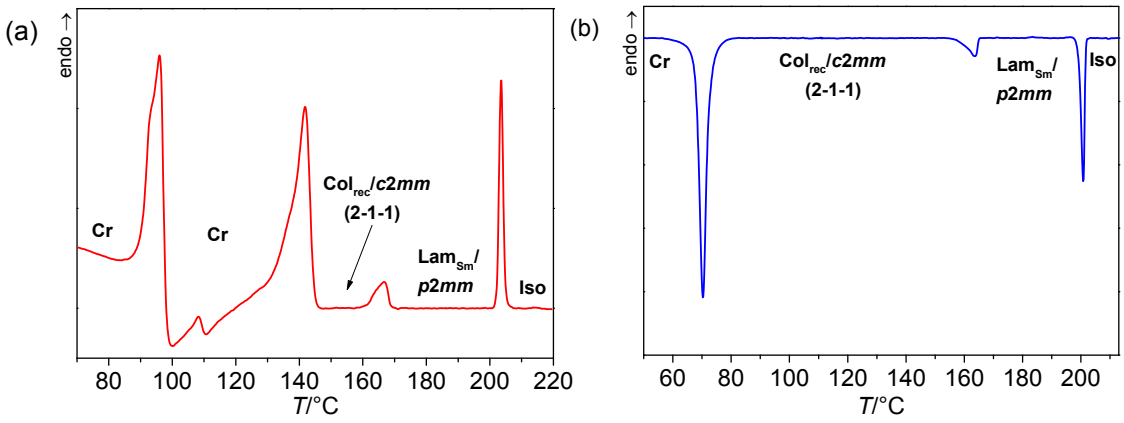

Figure S14. (a) DSC heating (there are several melting, crystallizations and Cr-Cr transitions) and (b) cooling scans of compound **1/32** at 10 K min^{-1} (second heating and cooling).

Table S9. Experimental and calculated *d*-spacings, relative integrated intensities, and phases used in the reconstruction of electron densities for the Col$_{rec}$/*c*2*mm*(2-1-1) phase of **1/32** at 105 ºC. All intensities values are Lorentz and multiplicity corrected.

(*hk*)	$d_{obs.}$- spacings (nm)	$d_{cal.}$- spacings (nm)	*Intensity*	*Phase*
(20)	5.90	5.90	53.1	π
(11)	4.22	4.22	100.0	π
(31)	2.96	2.97	12.2	0
(40)		2.95	24.4	0
(02)	2.26	2.26	24.7	0
(22)	2.11	2.11	8.2	0
(51)	2.09	2.09	6.6	π
(60)	1.97	1.97	4.5	π
(42)	1.79	1.79	3.5	π
(71)	1.58	1.58	1.5	0
(13)	1.49	1.49	2.2	π
(62)	1.48	1.48	0.7	0
(80)	1.47	1.48	0.6	π
(33)	1.40	1.41	0.2	0
(53)	1.27	1.27	0.6	0
(91)	1.26	1.26	0.1	π
a_{rec} = 11.80 nm, b_{rec} = 4.52 nm				

Table S10. Experimental and calculated *d*-spacings, relative integrated intensities, and phases used in the reconstruction of electron densities for the $Col_{rec}/p2mm$ phase of **1/32** at 170 ºC. All intensities values are Lorentz and multiplicity corrected.

(*hk*)	$d_{obs.}$- spacings (nm)	$d_{cal.}$- spacings (nm)	*Intensity*	*Phase*
(10)	4.06	4.06	100.0	π
(01)	2.18	2.18	0.3	π
(20)	2.03	2.03	6.0	0
a_{rec} = 4.06 nm, b_{rec} = 2.18 nm				

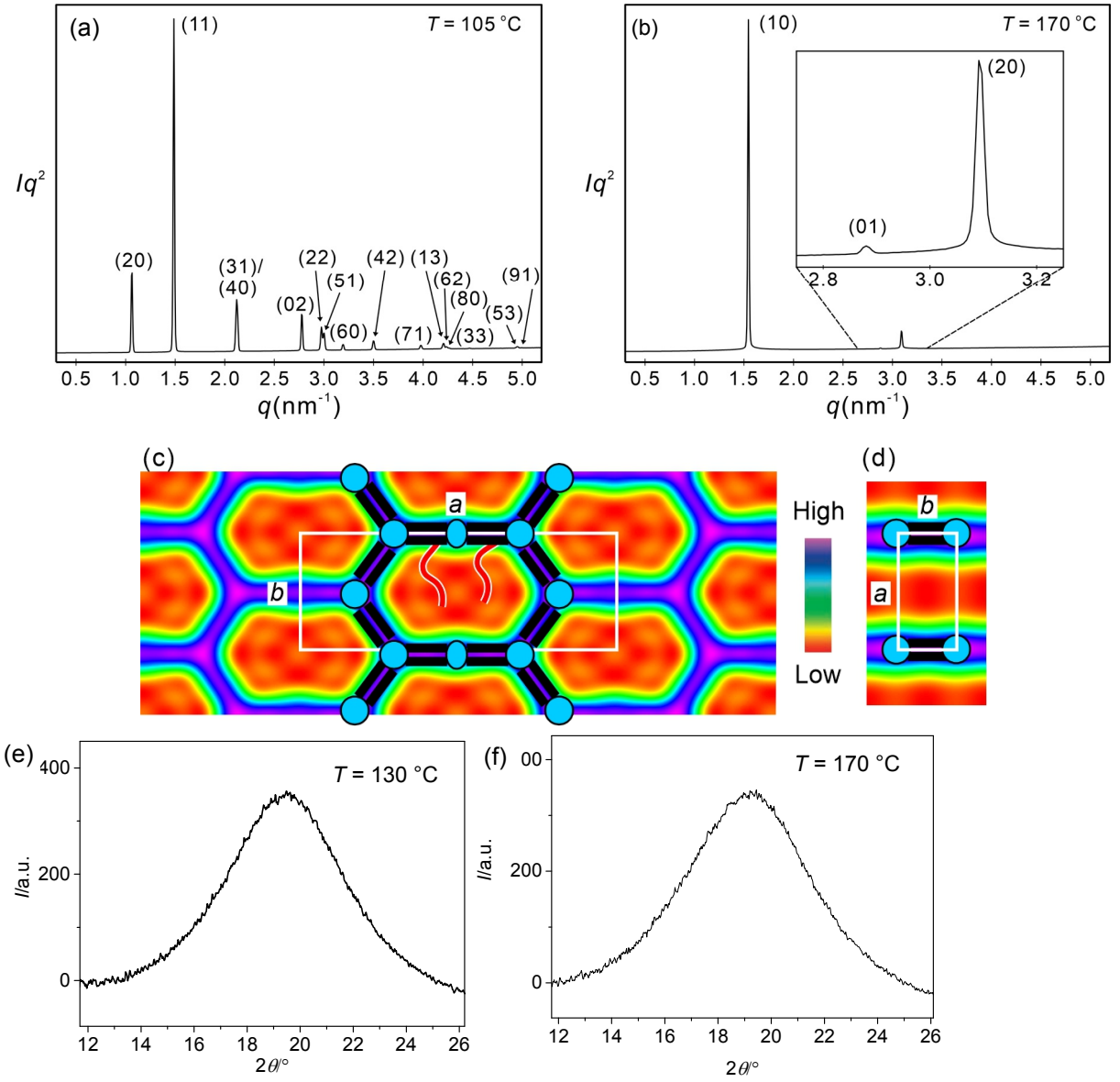

Figure S15. XRD of compound **1/32:** (a) SAXS diffractogram of the $Col_{rec}/c2mm$(2-1-1) phase at 105 ºC; (b) SAXS diffractogram of the $Lam_{Sm}/p2mm$ phase at 170 ºC with the corresponding electron density maps shown in (c) and (d), respectively; (c,d) WAXS in (e) in the $Col_{rec}/c2mm$ phase at 130 ºC and (f) in the $Lam_{Sm}/p2mm$ phase at 170 ºC.

2.7 Compound 1/34

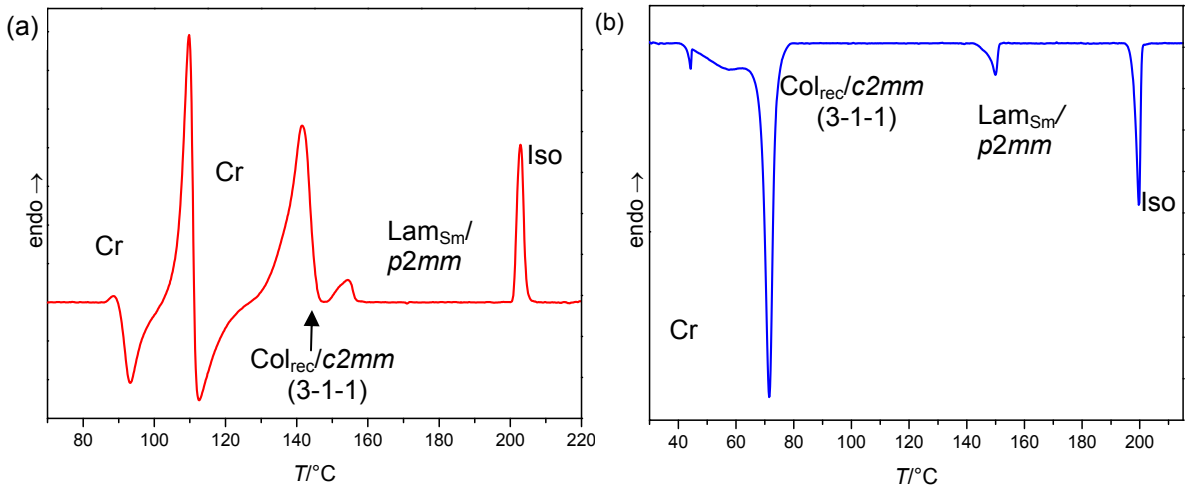

Figure S16. (a) DSC heating and (b) cooling scans of compound **1/34** at 10 K min^{-1} (first heating and cooling).

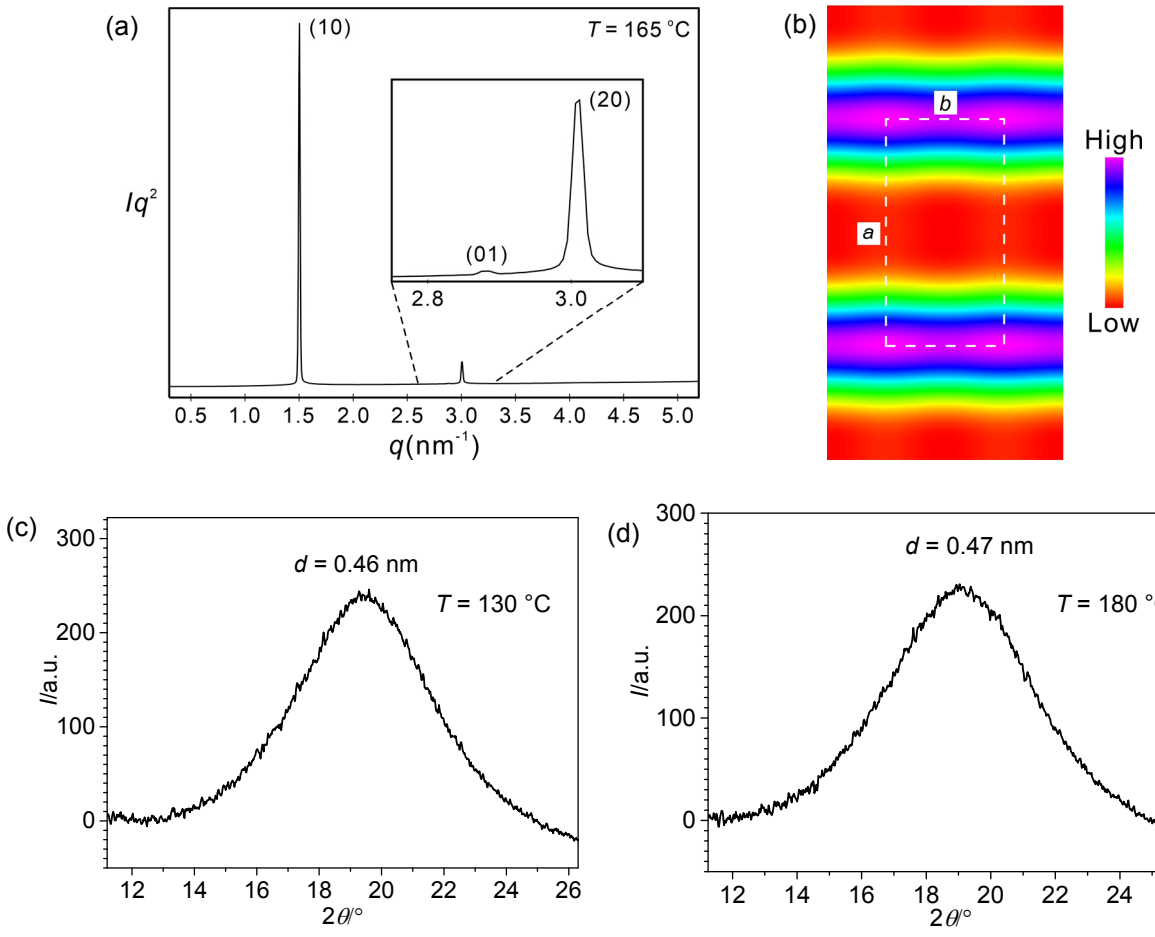

Figure S17. XRD of compound **1/34:** (a) SAXS diffractogram in the Lam$_{Sm}$/*p2mm* phase at 165 ºC with the corresponding electron density map shown in (b). (c,d) WAXS in (c) the Col$_{rec}$/*c2mm* phase at 130 ºC and (d) the Lam$_{Sm}$/*p2mm* phase at 180 ºC.

Table S11. Experimental and calculated *d*-spacings, relative integrated intensities, and phases used in the reconstruction of electron densities for the $Col_{rec}/c2mm$(3-1-1) phase of **1/34** at 105 ºC. All intensities values are Lorentz and multiplicity corrected.

(*hk*)	$d_{obs.}$- spacings (nm)	$d_{cal.}$- spacings (nm)	*Intensity*	*Phase*
(20)	8.11	8.11	30.7	π
(11)	4.35	4.35	100.0	π
(40)	4.06	4.06	21.3	0
(31)	3.47	3.47	10.7	0
(60)	2.70	2.70	11.7	π
(51)	2.63	2.64	4.4	π
(02)	2.26	2.26	24.4	0
(22)	2.17	2.18	4.4	π
(71)	2.06	2.06	3.5	/
(80)	2.03	2.03	2.0	/
(42)	1.97	1.97	3.2	/
(62)	1.73	1.73	1.3	/
(91)	1.67	1.67	1.1	/
(10/0)	1.62	1.62	0.4	/
(82)	1.51	1.51	0.5	/
(13)	1.50	1.50	2.0	/
(11/1)	1.40	1.40	0.2	/
(53)	1.36	1.37	0.1	/
(12/0)	1.35	1.35	0.1	/
(73)	1.26	1.26	0.3	/
a_{rec} = 16.22 nm, b_{rec} = 4.52 nm				

Table S12. Experimental and calculated *d*-spacings, relative integrated intensities, and phases used in the reconstruction of electron densities for the $Lam_{Sm}/p2mm$ phase of **1/34** at 165 ºC. All intensities values are Lorentz and multiplicity corrected.

(*hk*)	$d_{obs.}$- spacings (nm)	$d_{cal.}$- spacings (nm)	*Intensity*	*Phase*
(10)	4.18	4.18	100.0	π
(01)	2.18	2.18	0.1	π
(20)	2.09	2.09	7.1	0
a_{rec} =4.18 nm, b_{rec} = 2.18 nm				

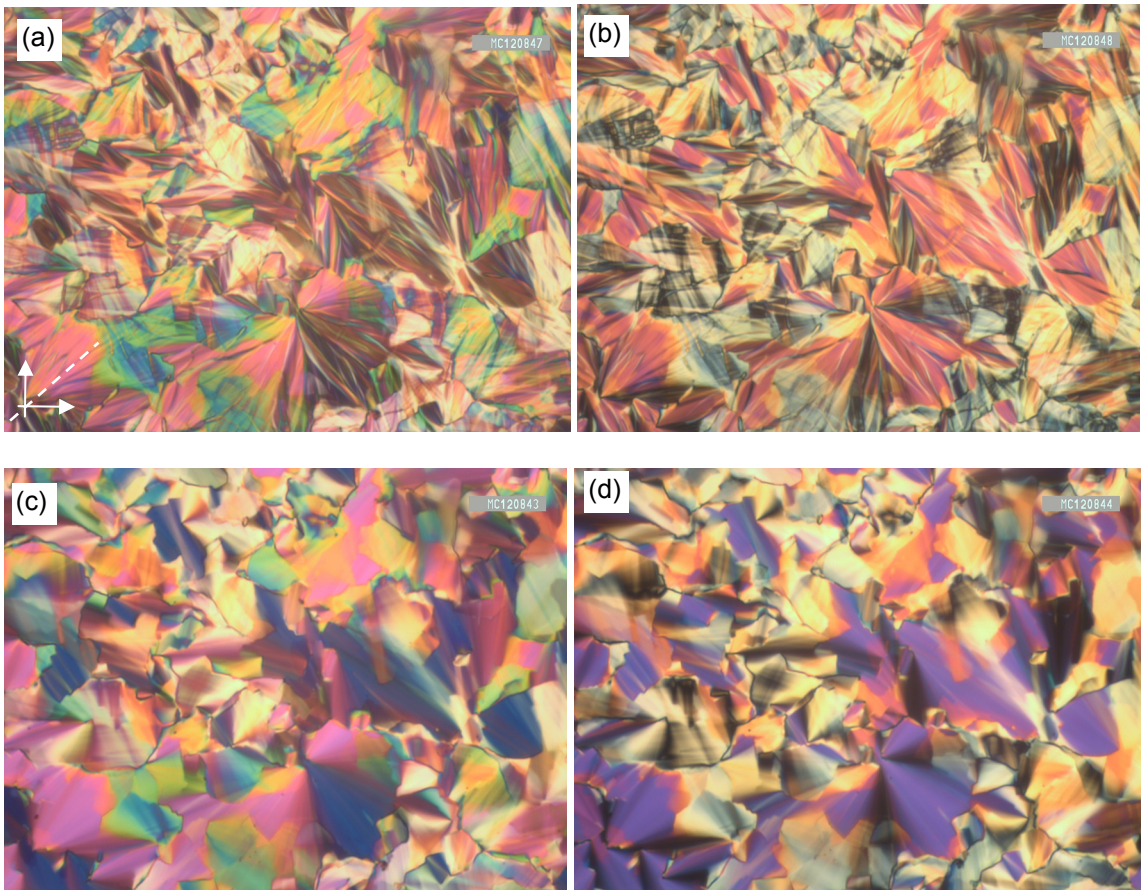

Figure S18. Optical textures of **1/34**, a,b) in the Lam_{Sm}/*p*2*mm* phase at 162 °C and (c,d) in the *c*2*mm*(3-1-1) giant honeycomb phase at 148 °C, as observed between crossed polarizers; (a,c) with, and (b,d) without λ-retarder plate. The directions of the polarizers (arrows) and the indicatrix (dashed line) of the λ-plate are shown in (a).

2.8 Structural data

Table S13. Lattice parameters and calculation of the molecular volume (V_{mol}), volume of the unit cells (V_{cell}), number of molecules in these unit cells (n_{cell}) and number of molecules in the lateral cross section of the honeycomb walls (n_{wall}).[a]

Compd.	Phase	T (°C)	a,b (nm)	d_{diff} (nm)	V_{cell}	V_R (nm^3)	V_{mol} (nm^3)	n_{cell}	n_{wall}
1/22	*p6mm*	150	a_{hex}= 4.46	0.46	7.92	0.56	1.07	6.6	2.2
1/24	*c2mm*	185	a=11.94; b=4.40	0.47	24.7	0.61	1.12	19.7	2.5
1/26	*c2mm*	170	a=12.02; b=4.41	0.47	24.9	0.66	1.17	19.0	2.4
1/28	*c2mm*	160	a=12.03; b=4.41	0.47	25.5	0.71	1.22	18.7	2.3
1/30	*c2mm*	160	a=11.80; b=4.45	0.46	24.2	0.76	1.27	17.0	2.1
1/32	*c2mm*	105	a=11.80; b=4.52	0.47	25.1	0.81	1.32	17.0	2.1
1/34	*c2mm*	105	a=16.22; b=4.52	0.46	33.7	0.86	1.37	22.0	2.2
1/24	*p2mm*	195	a=4.11; b=2.19	0.47	4.23	0.61	1.12	3.4	3.4
1/26	*p2mm*	200	a=3.91; b =2.20	0.47	4.04	0.66	1.17	3.1	3.1
1/28	*p2mm*	200	a=3.95; b= 2.19	0.47	4.07	0.71	1.22	3.0	3.0
1/32	*p2mm*	170	a=4.06; b=2.18	0.47	4.16	0.81	1.32	2.8	2.8
1/34	*p2mm*	165	a=4.18; b=2.18	0.46	4.19	0.86	1.37	2.7	2.7

[a] d_{diff}= maximum of the diffuse WAXS; V_{cell} = volume fraction of the lateral chain calculated from volume increments;[S1] $V_{cell} = A_{cell} \times h$, where $A_{cell} = a \times b$ for the rectangular phases and h corresponds to the d-value of the maximum of the diffuse wide angle scattering (d_{diff}). For the *p6mm* phases $A_{cell} = 0.866 \times a_{hex}^2$; V_{mol} = volume for a single molecule as calculated using crystal volume increments;[S1] n_{cell} = number of molecules in the unit cell, calculated according to $n_{cell} = k \times V_{cell}/V_{mol}$ with k = 0.893, being a correction for the packing density in the LC state;[S2,S3] n_{wall} = average number of molecules in the cross section of the honeycomb walls as from n_{cell} by dividing by the number of wall per unit cell (*p2mm*: 1; *p6mm*: 3; *c2mm*(2-1-1): 8, *c2mm*(3-1-1): 10) .

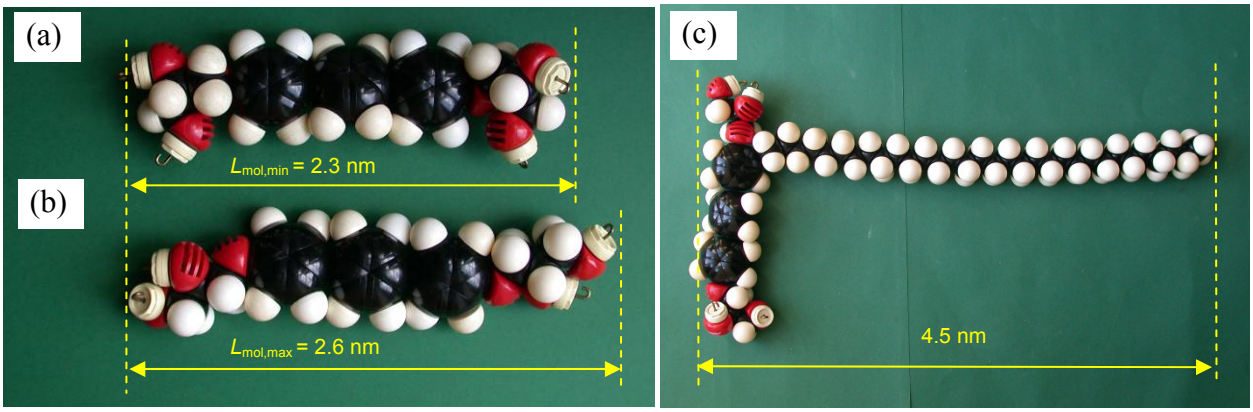

Figure S19. Molecular models showing compounds **1/*n*** (without lateral chain) in the conformations with a) minimized and b) maximized molecular length corresponding to $L_{mol,min}$ = 0.23 nm and $L_{mol,max}$ = 0.26 nm, respectively; c) shows **1/32** with *all-trans* chain.

3. Synthesis and analytical data

3.1 General

Synthesis of the compounds was performed according to Scheme S1 using the procedures described below. Unless otherwise noted, all starting materials were purchased from commercial sources and were used without further purification. Column chromatography was carried out with silica gel 60 (particle size 40-63 μm, or 63-200 μm, from Merck) and centrifugally-mediated chromatographic separation with gypsum-containing silica gel 60 (PF254, from Merck). Silica-coated aluminum foils (Kieselgel 60 F254, Merck) were used for thin-layer chromatography. Centrifugal-mediated chromatography was carried out with a chromatotron (Harrison Research). Flash chromatography was performed with a Büchi-Sepacore system. Determination of structures and purity of intermediates and products was obtained by NMR spectroscopy (VARIAN Gemini 2000 and Unity Inova 500, unless otherwise noted all spectra were recorded at 27 °C). Microanalyses were performed using a CARLO Erba-CHNO 1102 elemental analyzer. The purity of all products was checked with thin layer chromatography (silicagel 60 F254, Merck). $CHCl_3$/EtOAc mixtures and $CHCl_3$/MeOH mixtures were used as eluents and the spots were detected by UV radiation. All compounds represent racemic mixtures of diastereomers. The synthesis is outlined in Scheme, the synthesis of **2/0** and the experimental procedures are described in ref. [S3] and the analytical data of compounds **1/22-1/34** are collated in Section 3.3.
The long chain alcohols octacosanol, triacontanol and dotriacontanol were purchased from Shanghai Terppon and were used without further purification.

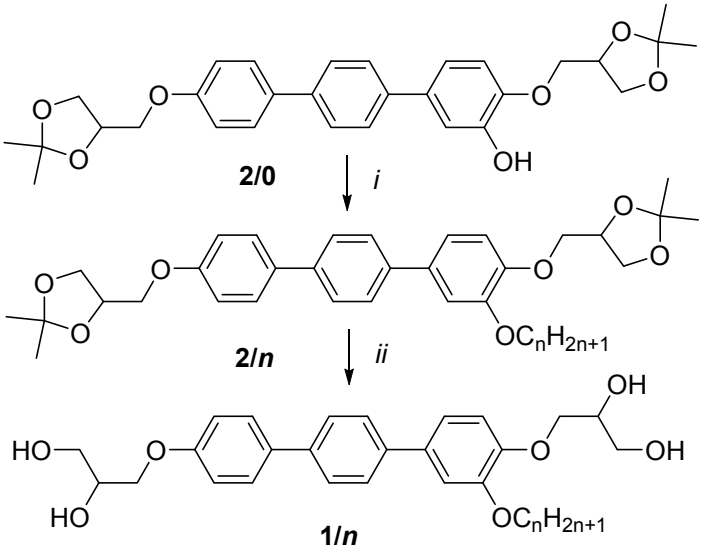

Scheme S1. Synthesis of compounds **1/*n***. *Regents and conditions*: i: $C_nH_{2n+1}Br$, K_2CO_3, acetonitrile, reflux, 5h; ii: MeOH, THF, cat. PPTS, 50 °C, 12 h.

3.2 Synthesis of long alkyl bromides and intermediates

Synthesis of the alkyl bromides with n = 24 and 26 is outlined in Scheme S2.

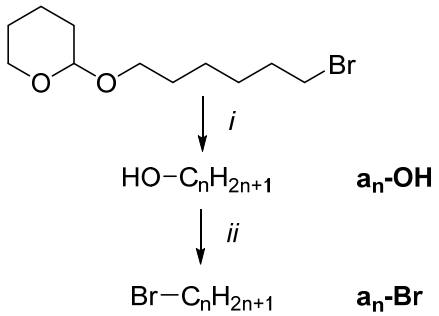

Scheme S2. Synthesis of compounds **a_{24}-Br** and **a_{26}-Br**. *Regents and conditions*: i: 1) Mg, THF, 55°C, 3h; 2) $C_nH_{2n+1}Br$, THF, -5 °C; 3) Li_2CuCl_4 solution (0.1 M in THF), -50 °C to RT, 2 + 12h; 4) cat. PPTS, reflux, 0.5 h; ii) method A) HBr (48%), H_2SO_4, Bu_4NHSO_4, *n*-hexane, reflux, 24h; method B) NBS, PPh_3, CH_2Cl_2, 20 °C, 12h.

General procedure for the preparation of long-chain alcohols a_n-OH

In a three-necked flask equipped with thermometer, reflux condenser and septum 1.5 eq magnesium turnings are placed and suspended with 80 mL dry THF under an argon atmosphere. To this suspension, 2- (6-bromohexyloxy) tetrahydro-2H-pyran (1 eq), dissolved in 10 mL THF, is added dropwise via the septum by means of a disposable syringe so that the temperature remains about 8 °C. In all cases, there is an advantage of dibromoethane etching. Subsequently, the reaction mixture is heated and kept at 55 °C for 3h. This Grignard reagent thus prepared is not isolated because the further reaction can be carried out directly with the crude product contained in the reaction mixture. The solution of the Grignard reagent is cooled to -5 ° C under an argon atmosphere using an ice / salt mixture and the corresponding bromoalkane (0.6 eq) dissolved in 15 mL of dry THF is added dropwise. Subsequently, the reaction mixture is cooled to -50 °C and 4 mL of a dilithium tetrachlorocuprate(II) solution (0.1 M in THF) was added. The reaction mixture is stirred for 2 h at this temperature and for a further 12 h at room temperature. Subsequently, carefully a saturated solution of ammonium chloride and 10% hydrochloric acid are added. This is followed by extraction three times with chloroform, the combined organic phases are dried over sodium sulfate and concentrated under reduced pressure to a volume of 100 mL. This enriched extract is treated with catalytic amounts of PPTS and heated for 0.5 h at reflux. Subsequently, the reaction mixture is concentrated under reduced pressure to complete dryness. The solid is purified by flash chromatography (eluent PE / EA 98: 2, v/v) and finally by crystallization from ethyl acetate.

General procedure for the preparation of long-chain alkyl bromides a_n-Br

Method A (for *n* = 24, 26). The corresponding alcohol a_n-OH (1 eq) is suspended in 30 ml of *n*-hexane and 50 ml of 48% aqueous HBr, treated with catalytic amounts of Bu4NHSO4 and concentrated sulfuric acid (2 mL) and heated to reflux for 24 h. The progress of the reaction is monitored by thin-layer chromatography. After the reaction is cooled to room temperature water is addes. This is followed by extraction three times with chloroform. The combined organic phases are washed with water and sat. sodium bicarbonate solution and then dried over sodium sulfate. After distilling off the solvent, the product is purified by flash chromatography (eluent PE / EA 98: 2, v/v).

Method B (for *n* = 28, 30, 32, 34). To a suspension of the corresponding alcohol a_n-OH (1 eq) in dry dichloromethane under argon atmosphere triphenylphosphine (1.2 eq) is added followed by N-bromosuccinimide (1.3 eq). The reaction mixture is stirred at room temperature and a change in color from yellow to orange to a deep red is observed. The mixture was allowed to stir overnight and the progress of the reaction is monitored by thin-

layer chromatography and quenched after the reaction with water. This is followed by extraction three times with dichloromethane. The combined organic phases are washed and dried over sodium sulfate. The solvent is evaporated under reduced pressure, the product is purified by flash chromatography (eluent PE / EA 98: 2, v/v).
For $n = 34$ dry DMF was used as solvent due to the insolubility in dichloromethane and the mixture was stirred at 80 °C for 24 h. The crude product was directly filtrated from the reaction mixture. The purification was done as described above (eluent: *n*-hexane).

Tetracosane-1-ol a_{24}-OH
Yield 72 %; colorless solid; m.p. 74-77 °C (lit. 75-76 °C)[S4], 357.7 g/mol; **^{1}H-NMR** ($CDCl_3$, 400 MHz): δ/ ppm = 3.62 (t, $^3J_{H,H}$ = 6.6 Hz, 2H, -CH_2-OH), 1.60 – 1.56 (m, 2H, -CH_2-CH_2-OH), 1.48 – 1.43 (m, 2H, -CH_2-CH_2-CH_2-OH), 1.43 – 1.19 (m, 40H, -CH_2-), 0.86 (t, $^3J_{H,H}$ = 6.7 Hz, 3H, -CH_3).

Hexacosane-1-ol a_{26}-OH
Yield 55 %; colorless solid; m.p. 79-84 °C (lit. 78-79 °C)[S4], 382.7 g/mol; **^{1}H-NMR** ($CDCl_3$, 400 MHz): δ/ ppm = 3.62 (t, $^3J_{H,H}$ = 6.6 Hz, 2H, -CH_2-OH), 1.60 – 1.55 (m, 2H, -CH_2-CH_2-OH), 1.48 – 1.43 (m, 2H, -CH_2-CH_2-CH_2-OH), 1.43 – 1.18 (m, 44H, -CH_2-), 0.86 (t, $^3J_{H,H}$ = 6.7 Hz, 3H, -CH_3).

1-Bromo-tetracosane a_{24}-Br
Yield 67 %; colorless solid; m.p. 53-56 °C (lit. 49-51 °C)[S5], 417.6 g/mol; **^{1}H-NMR** ($CDCl_3$, 400 MHz): δ/ ppm = 3.38 (t, $^3J_{H,H}$ = 4.7 Hz, 2H, -CH_2-Br), 1.91 – 1.80 (m, 2H, -CH_2-CH_2-Br), 1.47 – 1.17 (m, 42H, -CH_2-), 0.81 (t, $^3J_{H,H}$ = 6.7 Hz, 3H, -CH_3).

1-Bromo-hexacosane a_{26}-Br
Yield 65 %; colorless solid; m.p. 52-54 °C (lit. 54.5-55.5 °C)[S6], 445.60 g/mol; **^{1}H-NMR** ($CDCl_3$, 400 MHz): δ/ ppm = 3.40 (t, $^3J_{H,H}$ = 4.7 Hz, 2H, -CH_2-Br), 1.91 – 1.80 (m, 2H, -CH_2-CH_2-Br), 1.47 – 1.16 (m, 46H, -CH_2-), 0.81 (t, $^3J_{H,H}$ = 6.7 Hz, 3H, -CH_3).

1-Bromo-octacosane a_{28}-Br
Yield 96 %; colorless solid; m.p. 58-59 °C (lit. 59-59.5)[S6], 473.7 g/mol; **^{1}H-NMR** ($CDCl_3$, 400 MHz): δ/ ppm = 3.40 (t, $^3J_{H,H}$ = 6.6 Hz, 2H, -CH_2-Br), 1.91 – 1.80 (m, 2H, -CH_2-CH_2-Br), 1.47 – 1.16 (m, 50H, -CH_2-), 0.88 (t, $^3J_{H,H}$ = 7.1 Hz, 3H, -CH_3).

1-Bromo-triacontane a_{30}-Br
Yield 74 %; colorless solid; m.p. 64 °C; 501.7 g/mol; **^{1}H-NMR** ($CDCl_3$, 500 MHz): δ/ ppm = 3.40 (t, $^3J_{H,H}$ = 6.9 Hz, 2H, -CH_2-Br), 1.90 – 1.80 (m, 2H, -CH_2-CH_2-Br), 1.46 – 1.20 (m, 54H, -CH_2-), 0.88 (t, $^3J_{H,H}$ = 7.0 Hz, 3H, -CH_3).

1-Bromo-dotriacontane a_{32}-Br
Yield 97 %; colorless solid; m.p. 67-68 °C, 529.8 g/mol; **^{1}H-NMR** ($CDCl_3$, 400 MHz): δ/ ppm = 3.34 (t, $^3J_{H,H}$ = 7.0 Hz, 2H, -CH_2-Br), 1.91 – 1.80 (m, 2H, -CH_2-CH_2-Br), 1.47 – 1.17 (m, 58H, -CH_2-), 0.81 (t, $^3J_{H,H}$ = 7.1 Hz, 3H, -CH_3).

1-Bromo-tetratriacontane a_{34}-Br

Dimethyl 2-dotriacontylmalonate was synthesized according to the literature[S 7] from dimethyl malonate (9.4 g, 0.71 mol), 1-bromodotricontane (30.0 g, 0.57 mmol) and sodium hydride (2.6 g, 1.1 mol) in DMF (abs., 400 mL). Yield: 17.0 g (52%); colorless liquid; m.p. 76-77 °C; TLC (*n*-hexane/$CHCl_3$, 1/1 v/v); 580.1 g/mol, **^{1}H-NMR** ($CDCl_3$, 500 MHz): *δ*/ ppm

= 3.73 (s, 6H, -O-CH_3), 3.35 (t, $^3J_{H,H}$ = 7.6 Hz, 1H, -CH-), 1.94 – 1.83 (m, 2H, -CH-CH_2-), 1.47 – 1.02 (m, 60H, -CH_2-), 0.88 (t, $^3J_{H,H}$ = 6.8 Hz, 3H, -CH_3).

Methyl tetratriacantanoate was synthesized according to the literature[S7] from dimethyl 2-dotriacontylmalonate (17.0 g, 29.40 mmol), water (0.5 mL, 29.40 mmol) and lithium chloride (2.5 g, 58.7 mmol) in DMSO (abs., 250 mL). Yield: 7.0 g (46%); colorless liquid; m.p. 71-72 °C; TLC (*n*-hexane/$CHCl_3$, 1/1 v/v); 522.9 g/mol **^{1}H-NMR** ($CDCl_3$, 500 MHz): δ/ ppm = 3.67 (s, 3H, -O-CH_3), 2.34 (t, $^3J_{H,H}$ = 7.5 Hz, 2H, -C-CH_2), 1.70 – 1.56 (m, 2H, -C-CH$_2$-CH_2-), 1.37 – 1.04 (m, 60H, -CH_2-), 0.88 (t, $^3J_{H,H}$ = 6.8 Hz, 3H, -CH_3).

Tetratriacontanol was synthesized according to the literature[S7] from methyl tetratriacantanoate (7.0 g, 13.4 mmol) and $LiAlH_4$ (1.5 g, 40.2 mmol) in dry diethylether/THF, 2:1, 200 mL/ 100 mL). Yield: 3.4 g (51%); colorless solid; m.p. 93-94 °C; TLC ($CHCl_3$); 494.9 g/mol, **^{1}H-NMR** ($CDCl_3$, 500 MHz): δ/ ppm = 3.64 (q, $^3J_{H,H}$ = 5.5 Hz, 2H, HO-CH_2-), 1.60 – 1.54 (m, 2H, HO-CH$_2$-CH_2-), 1.43 – 1.05 (m, 62H, -CH_2-), 0.88 (t, $^3J_{H,H}$ = 7.0 Hz, 3H, -CH_3).

1-Bromo-tetratriacontane a_{34}-Br
Yield 90 %; colorless solid; m.p. 73-74 °C; 557.8 g/mol; **^{1}H-NMR** ($CDCl_3$, 500 MHz): δ/ppm = 3.41 (t, $^3J_{H,H}$ = 6.9 Hz, 2H, Br-CH_2-), 1.90 – 1.81 (m, 2H, Br-CH$_2$-CH_2-), 1.46 – 1.38 (m, 2H, Br-CH$_2$-CH$_2$-CH_2-), 1.36 – 1.05 (m, 60H, -CH_2-), 0.88 (t, $^3J_{H,H}$ = 6.9 Hz, 3H, -CH_3).

Preparation of compounds 2/*n*
A suspension of **2/0** (1.1 eq), the corresponding alkyl bromide **a_n-Br** (1 eq) and potassium carbonate (2 eq) are refluxed for six hours in anhydrous acetonitrile. The course of the reaction is monitored by thin-layer chromatography. After the reaction is cooled to room temperature, metered in water and then extracted with three times with diethyl ether, the combined organic phases are washed with sat. sodium chloride solution, then dried over sodium sulfate. After evaporating the solvent under reduced pressure, the purification is carried out by recrystallization from $CHCl_3$/PE or centrifugally-mediated chromatography (eluent $CHCl_3$).

4,4“-Bis[(2,2-dimethyl-1,3-dioxolane-4-yl)methoxy]-3-docosanyloxy-*p*-terphenyl 2/22
Yield 65 %; colorless solid; 815.17 g/mol; **^{1}H-NMR** ($CDCl_3$, 400 MHz): δ/ppm = 7.57 (s, 4H, Ar-*H*), 7.54 (d, $^3J_{H,H}$ = 8.9 Hz, 2H, Ar-*H*), 7.13 – 7.11 (m, 2H, Ar-*H*), 6.98 (dd, $^3J_{H,H}$ = 8.7 Hz, $^4J_{H,H}$ = 1.4 Hz, 3H, Ar-*H*), 4.56 – 4.47 (m, 2H, -OC*H*-), 4.19 – 3.96 (m, 9H, -OCH_2-), 3.91 (dd, $^3J_{H,H}$ = 8.5 Hz, $^3J_{H,H}$ = 5.4 Hz, 1H, -OCH_2-), 1.86 – 1.76 (m, 2H, -OCH$_2$CH_2-), 1.51 (s, 3H, -CH_3), 1.48 – 1.46 (m, 2H, -OCH$_2$CH$_2$CH_2-), 1.46 (s, 3H, -CH_3), 1.40 (s, 3H, -CH_3), 1.39 (s, 3H, -CH_3), 1.34 – 1.23 (m, 36H, -CH_2-), 0.86 (t, $^3J_{H,H}$ = 6.4 Hz, 3H, -CH_3).

4,4“-Bis[(2,2-dimethyl-1,3-dioxolane-4-yl)methoxy]-3-tetracosanyloxy-*p*-terphenyl 2/24
Yield 74 %; colorless solid; 843.22 g/mol; **^{1}H-NMR** ($CDCl_3$, 400 MHz): δ/ppm = 7.58 (s, 4H, Ar-*H*), 7.54 (d, $^3J_{H,H}$ = 8.9 Hz, 2H, Ar-*H*), 7.13 – 7.11 (m, 2H, Ar-*H*), 6.98 (dd, $^3J_{H,H}$ = 8.7 Hz, $^4J_{H,H}$ = 1.4 Hz, 3H, Ar-*H*), 4.56 – 4.47 (m, 2H, -OC*H*-), 4.19 – 3.96 (m, 9H, -OCH_2-), 3.91 (dd, $^3J_{H,H}$ = 8.5 Hz, $^3J_{H,H}$ = 5.4 Hz, 1H, -OCH_2-), 1.86 – 1.76 (m, 2H, -OCH$_2$CH_2-), 1.51 (s, 3H, -CH_3), 1.48 – 1.46 (m, 2H, -OCH$_2$CH$_2$CH_2-), 1.46 (s, 3H, -CH_3), 1.40 (s, 3H, -CH_3), 1.39 (s, 3H, -CH_3), 1.34 – 1.23 (m, 40H, -CH_2-), 0.86 (t, $^3J_{H,H}$ = 6.6 Hz, 3H, -CH_3).

4,4“-Bis[(2,2-dimethyl-1,3-dioxolane-4-yl)methoxy]-3-hexacosanyloxy-*p*-terphenyl 2/26
Yield 72 %; colorless solid; 871.3 g/mol; **^{1}H-NMR** ($CDCl_3$, 400 MHz): δ/ppm = 7.57 (s, 4H, Ar-*H*), 7.54 (d, $^3J_{H,H}$ = 8.7 Hz, 2H, Ar-*H*), 7.13 – 7.11 (m, 2H, Ar-*H*), 6.98 (dd, $^3J_{H,H}$ = 8.7

Hz, $^4J_{H,H}$ = 1.4 Hz, 3H, Ar-*H*), 4.56 – 4.47 (m, 2H, -OC*H*-), 4.19 – 3.96 (m, 9H, -OCH_2-), 3.91 (dd, $^3J_{H,H}$ = 8.5 Hz, $^3J_{H,H}$ = 5.4 Hz, 1H, -OCH_2-), 1.86 – 1.76 (m, 2H, -OCH$_2$CH_2-), 1.51 (s, 3H, -CH_3), 1.48 – 1.46 (m, 2H, -OCH$_2$CH$_2$CH_2-), 1.46 (s, 3H, -CH_3), 1.40 (s, 3H, -CH_3), 1.39 (s, 3H, -CH_3), 1.30 – 1.23 (m, 44H, -CH_2-), 0.86 (t, $^3J_{H,H}$ = 6.4 Hz, 3H, -CH_3).

4,4"-Bis[(2,2-dimethyl-1,3-dioxolane-4-yl)methoxy]-3-octacosanyloxy-*p*-terphenyl 2/28
Yield 72 %; colorless solid; 899.3 g/mol*;* **^{1}H-NMR** ($CDCl_3$, 400 MHz): δ/ppm = 7.58 (s, 4H, Ar-*H*), 7.54 (d, $^3J_{H,H}$ = 8.6 Hz, 2H, Ar-*H*), 7.13 – 7.11 (m, 2H, Ar-*H*), 6.98 (dd, $^3J_{H,H}$ = 7.4 Hz, $^4J_{H,H}$ = 1.6 Hz, 3H, Ar-*H*), 4.56 – 4.47 (m, 2H, -OC*H*-), 4.19 – 3.96 (m, 9H, -OCH_2-), 3.91 (dd, $^3J_{H,H}$ = 8.4 Hz, $^3J_{H,H}$ = 5.6 Hz, 1H, -OCH_2-), 1.86 – 1.76 (m, 2H, -OCH$_2$CH_2-), 1.51 (s, 3H, -CH_3), 1.48 – 1.46 (m, 2H, -OCH$_2$CH$_2$CH_2-), 1.46 (s, 3H, -CH_3), 1.40 (s, 3H, -CH_3), 1.39 (s, 3H, -CH_3), 1.30 – 1.23 (m, 48H, -CH_2-), 0.86 (t, $^3J_{H,H}$ = 6.8 Hz, 3H, -CH_3).

4,4"-Bis[(2,2-dimethyl-1,3-dioxolane-4-yl)methoxy]-3-triacontanyloxy-*p*-terphenyl 2/30
Yield 91 %; colorless solid; m.p. 92 °C; 927.3 g/mol*;* **^{1}H-NMR** ($CDCl_3$, 400 MHz): δ/ppm = 7.59 (s, 4H, Ar-*H*), 7.56 (d, $^3J_{H,H}$ = 8.7 Hz, 2H, Ar-*H*), 7.17 – 7.12 (m, 2H, Ar-*H*), 7.00 (dd, $^3J_{H,H}$ = 8.7 Hz, $^4J_{H,H}$ = 1.4 Hz, 3H, Ar-*H*), 4.55 – 4.47 (m, 2H, -OC*H*-), 4.23 – 3.97 (m, 9H, -OCH_2-), 3.93 (dd, $^3J_{H,H}$ = 8.5 Hz, $^3J_{H,H}$ = 5.8 Hz, 1H, -OCH_2-), 1.88 – 1.79 (m, 2H, -OCH$_2$CH_2-), 1.48 (s, 3H, -CH_3), 1.48 – 1.47 (m, 2H, -OCH$_2$CH$_2$CH_2-), 1.47 (s, 3H, -CH_3), 1.42 (s, 3H, -CH_3), 1.41 (s, 3H, -CH_3), 1.39 – 1.16 (m, 52H, -CH_2-), 0.88 (t, $^3J_{H,H}$ = 6.8 Hz, 3H, -CH_3).

4,4"-Bis[(2,2-dimethyl-1,3-dioxolane-4-yl)methoxy]-3-dotriacontanyloxy-*p*-terphenyl 2/32
Yield 87 %; colorless solid; m.p. 93-94 °C, 955.4 g/mol*;* **^{1}H-NMR** ($CDCl_3$, 400 MHz): δ/ppm = 7.58 (s, 4H, Ar-*H*), 7.54 (d, $^3J_{H,H}$ = 8.7 Hz, 2H, Ar-*H*), 7.13 – 7.11 (m, 2H, Ar-*H*), 6.98 (dd, $^3J_{H,H}$ = 7.4 Hz, $^4J_{H,H}$ = 1.6 Hz, 3H, Ar-*H*), 4.56 – 4.47 (m, 2H, -OC*H*-), 4.19 – 3.96 (m, 9H, -OCH_2-), 3.91 (dd, $^3J_{H,H}$ = 8.4 Hz, $^3J_{H,H}$ = 5.6 Hz, 1H, -OCH_2-), 1.86 – 1.76 (m, 2H, -OCH$_2$CH_2-), 1.51 (s, 3H, -CH_3), 1.48 – 1.46 (m, 2H, -OCH$_2$CH$_2$CH_2-), 1.46 (s, 3H, -CH_3), 1.40 (s, 3H, -CH_3), 1.39 (s, 3H, -CH_3), 1.32 – 1.23 (m, 56H, -CH_2-), 0.86 (t, $^3J_{H,H}$ = 6.6 Hz, 3H, -CH_3).

4,4"-Bis[(2,2-dimethyl-1,3-dioxolan-4-yl)methoxy]-3- tetratriacontanyloxy-*p*-terphenyl 2/34
Yield 85 %; colorless solid; m.p. 95-96 °C; 983.5 g/mol*;* **^{1}H-NMR** ($CDCl_3$, 400 MHz): δ/ppm = 7.60 (s, 4H, Ar-*H*), 7.58 – -7.53 (m, 2H, Ar-*H*), 7.17 – 7.12 (m, 2H, Ar-*H*), 7.03 – 6.97 (m, 3H, Ar-*H*), 4.56 – 4.46 (m, 2H, O-CH$_2$-C*H*-CH$_2$), 4.23 – 3.90 (m, 10 H, O-CH_2-CH-CH$_2$, O-CH$_2$-CH-CH_2, O-CH_2-CH$_2$), 1.88 – 1.79 (m, 2H, -OCH$_2$-CH_2-), 1.49 – 1.47 (m, 6H, -CH_3), 1.43-1.39 (m, 6H, -CH_3), 1.39 – 1.03 (m, 62H, -CH_2-), 0.88 (t, $^3J_{H,H}$ = 6.8 Hz, 3H, -CH_3).

3.3 Analytical data of compounds 1/22-1/34

Preparation of compounds 1/*n*
Compounds **1/n** were synthesized according to refs. [S8,S9]. A mixture of the appropriate isopropylidene acetal **2/n** (1 eq) and PPTS (tip of a spatula) in THF/MeOH(1:1, 40 mL/~5 mmol) was stirred at 50 °C for 12h. After finishing the reaction the solvent was removed under reduced pressure and the residue was solved in DCM. The organic layer was washed with sat. $NaHCO_3$ solution (3x50 mL) and brine. After drying over Na_2SO_4 the solvent was removed and the residue purified by column chromatography (eluent: $CHCl_3$/MeOH = 9/1, v/v) ad recrystallization from MeOH/THF.

4,4"-Bis(2,3-dihydroxypropyloxy)-3-docosanyloxy-*p*-terphenyl (1/22)
Yield 87 %; colorless solid; for transition temperatures, see Table 1; 735.0 g/mol; **^{1}H-NMR** (pyridine-d_5, 400 MHz): δ/ppm = 7.82 (d, $^3J_{H,H}$ = 8.4 Hz, 2H, Ar-*H*), 7.78 (d, $^3J_{H,H}$ = 7.5 Hz, 2H, Ar-*H*), 7.70 (d, $^3J_{H,H}$ = 8.7 Hz, 2H, Ar-*H*), 7.49 (d, $^4J_{H,H}$ = 2.0 Hz, 1H, Ar-*H*), 7.36 (dd, $^3J_{H,H}$ = 6.3 Hz, $^4J_{H,H}$ = 2.1 Hz, 1H, Ar-*H*), 7.28 (d, $^3J_{H,H}$ = 8.4 Hz, 1H, Ar-*H*), 7.21 (s, 1H, Ar-*H*), 7.19 – 7.18 (m, 1H, Ar-*H*, covered by pyridine signals), 4.61 – 4.46 (m, 5H, -OC*H*-, -OCH_2-), 4.45 (dd, $^3J_{H,H}$ = 9.2 Hz, $^3J_{H,H}$ = 5.6 Hz, 1H, -OCH_2-), 4.27 (dd, $^2J_{H,H}$ = 6.2 Hz, $^3J_{H,H}$ = 4.4 Hz, 2H, -OCH_2-), 4.19 – 4.16 (m, 4H, -OCH_2-), 1.89 – 1.83 (m, 2H, -OCH$_2$CH_2-), 1.57 – 1.50 (m, 2H, -OCH$_2$CH$_2$CH_2-), 1.33 – 1.31 (m, 36H, -CH_2-), 0.88 (t, $^3J_{H,H}$ = 6.7 Hz, 3H, -CH_3); **^{13}C-NMR** (pyridine-d_5, 125 MHz, 50°C): *δ*/ppm = 159.7, 150.5, 150.1 (covered by pyridine signals), 139.8, 139.7, 134.7, 133.5, 128.4, 127.6, 127.4, 123.8, 123.1, 120.1, 115.9, 115.8, 114.0, 72.7, 71.6, 71.6, 71.2, 69.9, 64.7, 64.4, 32.2, 30.0, 29.8, 29.6, 26.5, 22.9, 14.2. **Elemental analysis**: calcd. for $C_{46}H_{70}O_7$: C 75.16%; H 9.60%; found: C 75.07%; H 9.57%.

4,4"-Bis(2,3-dihydroxypropyloxy)-3-tetracosanyloxy-*p*-terphenyl (1/24)
Yield 92 %; colorless solid; transition temperatures, see Table 1; 762.5 g/mol; **^{1}H-NMR** (pyridine-d_5, 400 MHz, 50°C): δ/ppm = 7.82 (d, $^3J_{H,H}$ = 8.1 Hz, 2H, Ar-*H*), 7.77 (d, $^3J_{H,H}$ = 8.2 Hz, 2H, Ar-*H*), 7.70 (d, $^3J_{H,H}$ = 8.5 Hz, 2H, Ar-*H*), 7.50 (d, $^4J_{H,H}$ = 1.7 Hz, 1H, Ar-*H*), 7.35 (dd, $^3J_{H,H}$ = 8.2 Hz, $^4J_{H,H}$ = 1.7 Hz, 1H, Ar-*H*), 7.28 (d, $^3J_{H,H}$ = 8.2 Hz, 1H, Ar-*H*), 7.21 (s, 1H, Ar-*H*), 7.20 – 7.19 (m, 1H, Ar-*H*, covered by pyridine signals), 4.60 – 4.51 (m, 5H, -OC*H*-, -OCH_2-), 4.45 (dd, $^3J_{H,H}$ = 9.0 Hz, $^3J_{H,H}$ = 5.6 Hz, 1H, -OCH_2-), 4.26 (dd, $^3J_{H,H}$ = 6.1 Hz, $^3J_{H,H}$ = 4.4 Hz, 2H, -OCH_2-), 4.19 – 4.16 (m, 4H, -OCH_2-), 1.88 – 1.84 (m, 2H, -OCH$_2$CH_2-), 1.58 – 1.51 (m, 2H, -OCH$_2$CH$_2$CH_2-), 1.34 – 1.31 (m, 40H, -CH_2-), 0.88 (t, $^3J_{H,H}$ = 7.2 Hz, 3H, -CH_3); **^{13}C-NMR** (pyridine-d_5, 125 MHz, 50°C): *δ*/ppm = 159.6, 150.5, 149.7 (covered by pyridine signals), 139.8, 139.6, 134.6, 133.5, 128.3, 127.6, 127.3, 120.1, 115.9, 115.7, 113.9, 72.6, 71.5, 71.5, 71.1, 69.9, 64.6, 64.4, 32.1, 30.0, 29.9, 29.7, 29.5, 26.4, 22.9, 14.7. **Elemental analysis**: calcd. for $C_{48}H_{74}O_7$: C 75.55%; H 9.77% found: C 75.85%; H 10.02%.

4,4"-Bis(2,3-dihydroxypropyloxy)-3-hexacosanyloxy-*p*-terphenyl (1/26)
Yield 90 %; colorless solid; transition temperatures, see Table 1; 790.6 g/mol; **^{1}H-NMR** (pyridine-d_5, 400 MHz, 50°C): δ/ppm = 7.83 (d, $^3J_{H,H}$ = 8.4 Hz, 2H, Ar-*H*), 7.78 (d, $^3J_{H,H}$ = 8.4 Hz, 2H, Ar-*H*), 7.71 (d, $^3J_{H,H}$ = 8.5 Hz, 2H, Ar-*H*), 7.50 (d, $^4J_{H,H}$ = 2.0 Hz, 1H, Ar-*H*), 7.35 (dd, $^3J_{H,H}$ = 8.2 Hz, $^4J_{H,H}$ = 2.0 Hz, 1H, Ar-*H*), 7.29 (d, $^3J_{H,H}$ = 8.4 Hz, 1H, Ar-*H*), 7.22 (s, 1H, Ar-*H*), 7.19 – 7.20 (m, 1H, Ar-*H*, covered by pyridine signals), 4.61 – 4.54 (m, 5H, -OC*H*-, -OCH_2-), 4.47 (dd, $^3J_{H,H}$ = 8.8 Hz, $^3J_{H,H}$ = 5.5 Hz, 1H, -OCH_2-), 4.25 (dd, $^3J_{H,H}$ = 6.2 Hz, $^3J_{H,H}$ = 4.4 Hz, 2H, -OCH_2-), 4.18 – 4.14 (m, 4H, -OCH_2-), 1.88 – 184 (m, 2H, -OCH$_2$CH_2-), 1.52 – 1.49 (m, 2H, -OCH$_2$CH$_2$CH_2-), 1.32 – 1.30 (m, 44H, -CH_2-), 0.85 (t, $^3J_{H,H}$ = 6.7 Hz, 3H, -CH_3); **^{13}C-NMR** (pyridine-d_5, 125 MHz, 50°C): *δ*/ppm = 159.7, 150.5, 150.2 (covered by pyridine signals), 139.8, 139.7, 134.7, 133.5, 128.4, 127.6, 127.4, 120.1, 115.9, 115.8, 114.0, 72.7, 71.6, 71.6, 71.2, 69.9, 64.7, 64.4, 32.2, 30.0, 30.0, 29.9, 29.8, 29.6, 26.5, 22.9, 14.2. **Elemental analysis**: calcd. for $C_{50}H_{78}O_7 \cdot 0.5\ H_2O$: C 75.05%; H 9.95% found: C 74.91%; H 9.82%.

4,4"-Bis(2,3-dihydroxypropyloxy)-3-octacosanyloxy-*p*-terphenyl (1/28)
Yield 83 %; colorless solid; transition temperatures, see Table 1; 818.6 g/mol; **1H-NMR** (pyridine-d_5, 400 MHz, 50°C): δ/ppm = 7.80 (d, $^3J_{H,H}$ = 8.4 Hz, 2H, Ar-*H*), 7.78 (d, $^3J_{H,H}$ = 8.4 Hz, 2H, Ar-*H*), 7.71 (d, $^3J_{H,H}$ = 8.7 Hz, 2H, Ar-*H*), 7.50 (d, $^4J_{H,H}$ = 2.0 Hz, 1H, Ar-*H*), 7.36 (dd, $^3J_{H,H}$ = 8.4 Hz, $^4J_{H,H}$ = 2.1 Hz, 1H, Ar-*H*), 7.29 (d, $^3J_{H,H}$ = 8.4 Hz, 1H, Ar-*H*), 7.22 (s, 1H, Ar-*H*), 7.19 – 7.20 (m, 1H, Ar-*H*, covered by pyridine signals), 4.61 – 4.52 (m, 5H, -OC*H*-, -OCH_2-), 4.46 (dd, $^3J_{H,H}$ = 9.0 Hz, $^3J_{H,H}$ = 5.5 Hz, 1H, -OCH_2-), 4.26 (dd, $^3J_{H,H}$ = 6.1

Hz, $^3J_{H,H}$ = 4.4 Hz, 2H, -OCH_2-), 4.22 – 4.19 (m, 4H, -OCH_2-), 1.89 – 1.86 (m, 2H, -OCH$_2$CH_2-), 1.56 – 1.53 (m, 2H, -OCH$_2$CH$_2$CH_2-), 1.35 – 1.32 (m, 48H, -CH_2-), 0.89 (t, $^3J_{H,H}$ = 6.9 Hz, 3H, -CH_3); **^{13}C-NMR** (pyridine-d$_5$, 125 MHz, 50°C): *δ*/ppm = 159.6, 150.5, 149.7 (covered by pyridine signals), 139.8, 139.6, 134.6, 133.5, 128.3, 127.6, 127.3, 120.1, 115.9, 115.7, 113.9, 72.6, 71.5, 71.5, 71.1, 69.9, 64.6, 64.4, 32.1, 30.0, 29.9, 29.9, 29.7, 29.6, 26.4, 22.9, 14.6. **Elemental analysis**: calcd. for $C_{52}H_{82}O_7$: C 76.24%; H 10.09%; found: C 76.18%; H 9.75%.

4,4"-Bis(2,3-dihydroxypropyloxy)-3-triacontanyloxy-*p*-terphenyl (1/30)
Yield 32 %; colorless solid; transition temperatures, see Table 1; 847.3 g/ mol; **^{1}H-NMR** (pyridine-d$_5$, 400 MHz): δ/ppm = 7.87 (d, $^3J_{H,H}$ = 8.4 Hz, 2H, Ar-*H*), 7.81 (d, $^3J_{H,H}$ = 8.4 Hz, 2H, Ar-*H*), 7.74 (d, $^3J_{H,H}$ = 8.7 Hz, 2H, Ar-*H*), 7.53 (d, $^4J_{H,H}$ = 2.0 Hz, 1H, Ar-*H*), 7.39 (dd, $^3J_{H,H}$ = 8.3 Hz, $^4J_{H,H}$ = 2.0 Hz, 1H, Ar-*H*), 7.32 (d, $^3J_{H,H}$ = 8.4 Hz, 1H, Ar-*H*), 7.25 (s, 1H, Ar-*H*), 7.24 – 7.23 (m, 1H, Ar-*H*, covered by pyridine signals), 4.70 – 4.55 (m, 5H, -OC*H*-, -OCH_2-), 4.50 (dd, $^3J_{H,H}$ = 9.3 Hz, $^3J_{H,H}$ = 6.0 Hz, 1H, -OCH_2-), 4.39 – 4.24 (m, 4H, -OCH_2-), 4.18 (t, $^3J_{H,H}$ = 6.5 Hz, 2H, -OCH_2-), 1.90 – 1.81 (m, 2H, -OCH$_2$CH_2-), 1.58 – 1.48 (m, 2H, -OCH$_2$CH$_2$CH_2-), 1.39 – 1.21 (m, 52H, -CH_2-), 0.88 (t, $^3J_{H,H}$ = 6.8 Hz, 3H, -CH_3); **^{13}C-NMR** (pyridine-d$_5$, 125 MHz) *δ*/ppm = 160.5, 150.5, 149.7 (covered by pyridine signals), 140.6, 140.5, 135.3, 134.2, 129.2, 128.5, 128.2, 120.8, 116.5, 116.2, 73.3, 72.4, 72.0, 70.5, 65.5, 65.3, 33.0, 30.9, 30.8, 30.7, 30.5, 27.3, 23.8, 15.2. **Elemental analysis**: calcd. for $C_{54}H_{86}O_7 \cdot 0.5\ H_2O$: C 75.75%; H 10.24%; found: C 75.98%; H 10.30%.

4,4"-Bis(2,3-dihydroxypropyloxy)-3-dotriacontanyloxy-*p*-terphenyl (1/32)
Yield 84 %; colorless solid; transition temperatures, see Table 1; 874.7 g/mol; **^{1}H-NMR** (pyridine-d$_5$, 400 MHz, 80°C): δ/ppm = 7.83 (d, $^3J_{H,H}$ = 8.3 Hz, 2H, Ar-*H*), 7.78 (d, $^3J_{H,H}$ = 8.2 Hz, 2H, Ar-*H*), 7.71 (d, $^3J_{H,H}$ = 8.5 Hz, 2H, Ar-*H*), 7.50 (d, $^4J_{H,H}$ = 1.8 Hz, 1H, Ar-*H*), 7.37 (dd, $^3J_{H,H}$ = 8.4 Hz, $^4J_{H,H}$ = 1.6 Hz, 1H, Ar-*H*), 7.29 (d, $^3J_{H,H}$ = 8.2 Hz, 1H, Ar-*H*), 7.22 (s, 1H, Ar-*H*), 7.20 – 7.19 (m, 1H, Ar-*H*, covered by pyridine signals), 4.64 – 4.51 (m, 5H, -OC*H*-, -OCH_2-), 4.46 (dd, $^3J_{H,H}$ = 9.2 Hz, $^3J_{H,H}$ = 5.8 Hz, 1H, -OCH_2-), 4.32 – 4.15 (m, 6H, -OCH_2-), 1.90 – 1.81 (m, 2H, -OCH$_2$CH_2-), 1.58 – 1.49 (m, 2H, -OCH$_2$CH$_2$CH_2-), 1.48 – 1.11 (m, 56H, -CH_2-), 0.88 (t, $^3J_{H,H}$ = 6.5 Hz, 3H, -CH_3); **^{13}C-NMR** (pyridine-d$_5$, 125 MHz, 50°C): δ/ppm = 159.6, 150.5, 149.7 (covered by pyridine signals), 139.8, 139.7, 135.5, 133.5, 128.1, 127.3, 127.1, 119.8, 115.4, 115.7, 113.5, 72.3, 71.3, 70.9, 71.2, 69.6, 64.4, 64.1, 32.1, 30.0, 29.9, 29.9, 29.7, 29.5, 26.2, 22.7, 14.3. **Elemental analysis**: calcd. for $C_{56}H_{90}O_7 \cdot H_2O$: C 75.62%; H 10.24%; found: C 75.47%; H 10.27%.

4,4"-Bis(2,3-dihydroxypropyloxy)-3-tetracontanyloxy-*p*-terphenyl (1/34)
Yield 38 %; colorless solid; transition temperatures, see Table 1; 903.4 g/mol; **^{1}H-NMR** (pyridine-d$_5$, 400 MHz, 80°C): δ/ppm = 7.82 (d, $^3J_{H,H}$ = 8.1 Hz, 2H, Ar-*H*), 7.77 (d, $^3J_{H,H}$ = 8.3 Hz, 2H, Ar-*H*), 7.71 (d, $^3J_{H,H}$ = 8.6 Hz, 2H, Ar-*H*), 7.51 (d, $^4J_{H,H}$ = 1.8 Hz, 1H, Ar-*H*), 7.37 (dd, $^3J_{H,H}$ = 8.3 Hz, $^4J_{H,H}$ = 1.8 Hz, 1H, Ar-*H*), 7.29 (d, $^3J_{H,H}$ = 8.3 Hz, 1H, Ar-*H*), 7.22 (s, 1H, Ar-*H*), 7.21 – 7.20 (m, 1H, Ar-*H*, covered by pyridine signals), 4.61 – 4.49 (m, 5H, -OC*H*-, -OCH_2-), 4.44 (dd, $^3J_{H,H}$ = 11.1 Hz, $^3J_{H,H}$ = 7.6 Hz, 1H, -OCH_2-), 4.28 - 4.13 (m, 6H, -OCH_2-), 1.95 – 1.86 (m, 2H, -OCH$_2$CH_2-), 1.63 – 1.55 (m, 2H, -OCH$_2$CH$_2$CH_2-), 1.54 – 1.19 (m, 60H, -CH_2-), 0.93 (t, $^3J_{H,H}$ = 6.8 Hz, 3H, -CH_3); **^{13}C-NMR** (pyridine-d$_5$, 125 MHz): *δ*/ppm = 159.7, 150.7, 150.1 (covered by pyridine signals), 139.8, 139.7, 135.5, 133.7, 128.3, 127.5, 127.3, 120.2, 116.4, 115.9, 114.4, 72.9, 71.6, 71.5, 71.2, 70.2, 64.6, 64.4, 32.1, 29.9, 29.7, 29.5, 26.5, 22.8, 14.1. **Elemental analysis**: calcd. for $C_{58}H_{94}O_7 \cdot H_2O$: C 75.92%; H 10.37%; found: C 75.92%; H 10.36%.

3.4 Representative NMR spectra

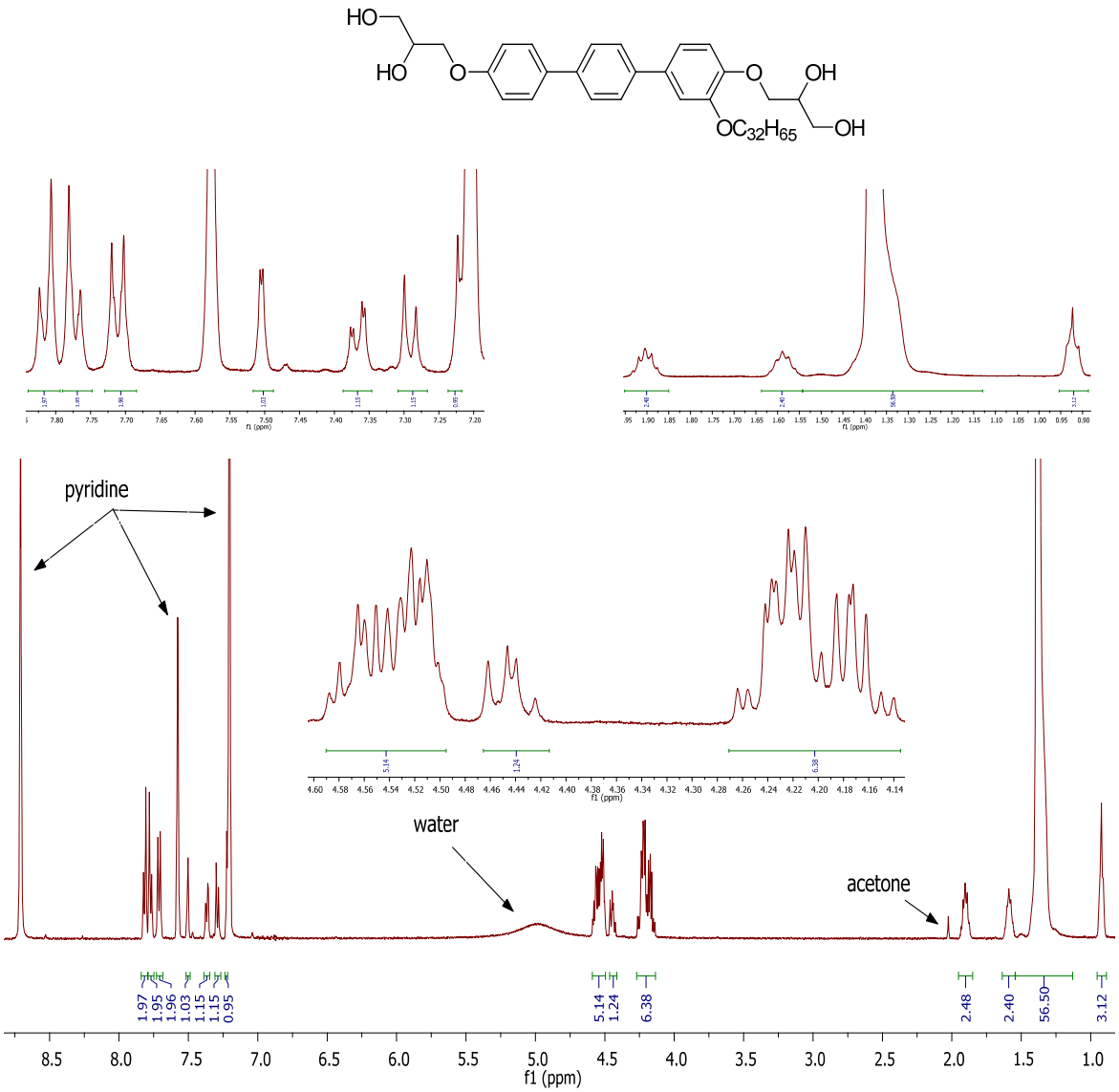

Figure S20. 1H-NMR spectrum of compound **1/32** in pyridine-d_5 at 80 °C (400 MHz)

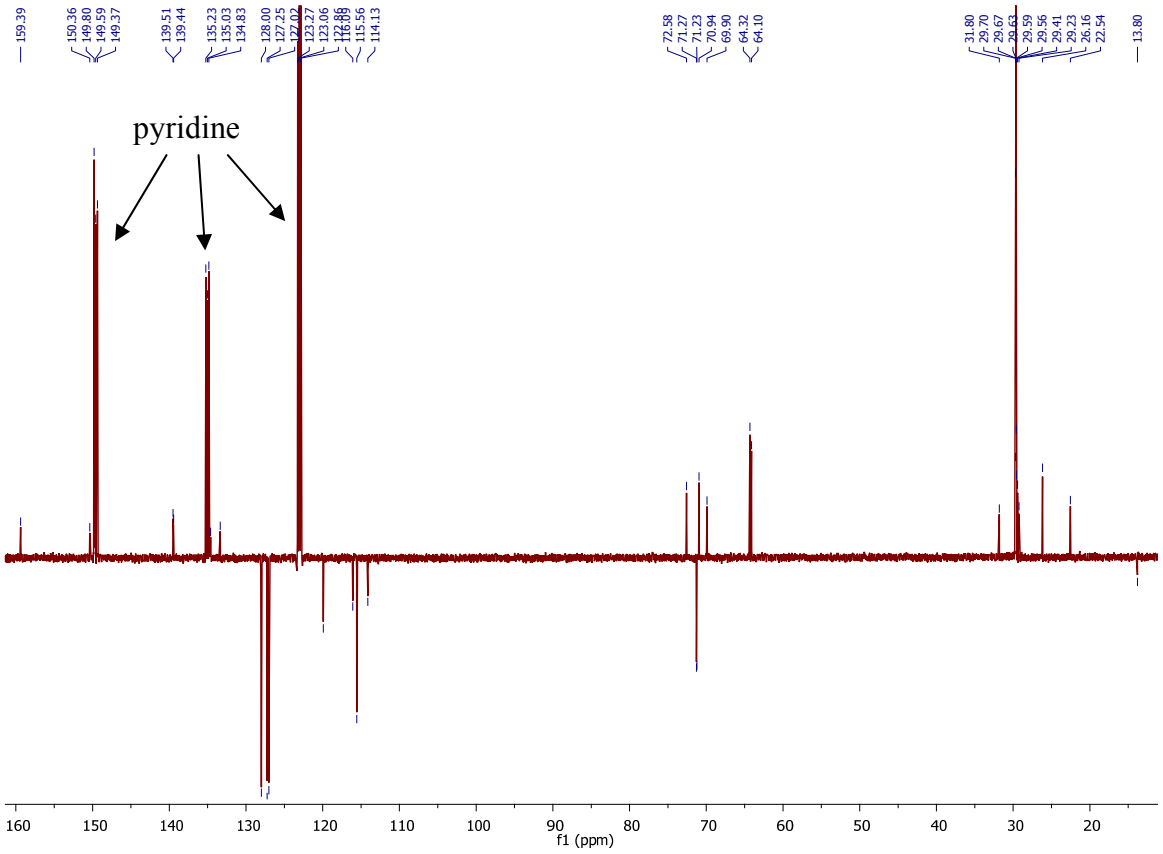

Figure S21. ^{13}C-NMR spectrum of compound **1/32** in pyridine-d_5 at 80 °C (125 MHz).

4. References

S1 A. Immirizi, B. Perini, *Acta Cryst.*, 1977, **A33**, 216-218.

S2 A. I. Kitaigorodski, *Molekülkristalle*, Akademieverlag: Berlin, Germany, 1979.

S3 A. Lehmann, M. Prehm, F. Liu, X. B. Zeng, G. Ungar and C. Tschierske, *Chem. Commun.,* 2018, **54**, 12306—12309.

S4 L. I. Zakharkin, I. M. Churilova and E. V. Anikina, *Zh. Org. Khim*., 1988, **24**, 77.

S5 R. Al Dulayymi, M. S. Baird and E. Roberts, *Tetrahedron,* 2005, **61**, 11939-11951.

S6 J. E. Hesse, *J. Chem. Eng. Data*, 1967, **12**, 266.

S7 S. Poppe, A. Lehmann, A. Scholte, M. Prehm, X. Zeng, G. Ungar and C. Tschierske, *Nat. Commun.,* 2015, **6**, 8637.

S8 S. Poppe, M. Poppe, H. Ebert, M. Prehm, C. Chen, F. Liu, S. Werner, K. Bacia and C. Tschierske, *Polymers,* 2017, **9**, 471.

S9 R. van Rijsbergen, M.-J. Anteunis and A. de Bruyn, *J. Carbohydr. Chem.,* 2006, **2**, 395-404.